
CHAPTER 3

VIBRATION OF A RESILIENTLY SUPPORTED RIGID BODY

Harry Himelblau
Sheldon Rubin

INTRODUCTION

This chapter discusses the vibration of a rigid body on resilient supporting elements, including (1) methods of determining the inertial properties of a rigid body, (2) discussion of the dynamic properties of resilient elements, and (3) motion of a single rigid body on resilient supporting elements for various dynamic excitations and degrees of symmetry.

The general equations of motion for a rigid body on linear massless resilient supports are given; these equations are general in that they include any configuration of the rigid body and any configuration and location of the supports. They involve six simultaneous equations with numerous terms, for which a general solution is impracticable without the use of high-speed automatic computing equipment. Various degrees of simplification are introduced by assuming certain symmetry, and results useful for engineering purposes are presented. Several topics are considered: (1) determination of undamped natural frequencies and discussion of coupling of modes of vibration; (2) forced vibration where the excitation is a vibratory motion of the foundation; (3) forced vibration where the excitation is a vibratory force or moment generated within the body; and (4) free vibration caused by an instantaneous change in velocity of the system (velocity shock). Results are presented mathematically and, where feasible, graphically.

SYSTEM OF COORDINATES

The motion of the rigid body is referred to a fixed "inertial" frame of reference. The inertial frame is represented by a system of cartesian coordinates $\bar{X}, \bar{Y}, \bar{Z}$. A similar system of coordinates X, Y, Z fixed in the body has its origin at the center-of-mass. The two sets of coordinates are coincident when the body is in equilibrium under the

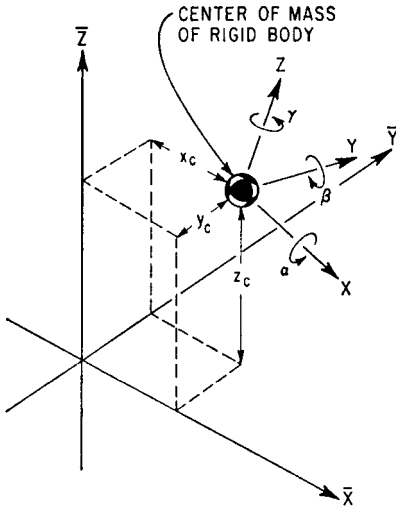


FIGURE 3.1 System of coordinates for the motion of a rigid body consisting of a fixed inertial set of reference axes ($\bar{X}, \bar{Y}, \bar{Z}$) and a set of axes (X, Y, Z) fixed in the moving body with its origin at the center-of-mass. The axes $\bar{X}, \bar{Y}, \bar{Z}$ and X, Y, Z are coincident when the body is in equilibrium under the action of gravity alone. The displacement of the center-of-mass is given by the translational displacements x_c, y_c, z_c and the rotational displacements α, β, γ as shown. A positive rotation about an axis is one which advances a right-handed screw in the positive direction of the axis.

action of gravity alone. The motions of the body are described by giving the displacement of the body axes relative to the inertial axes. The translational displacements of the center-of-mass of the body are x_c, y_c, z_c in the $\bar{X}, \bar{Y}, \bar{Z}$ directions, respectively. The rotational displacements of the body are characterized by the angles of rotation α, β, γ of the body axes about the $\bar{X}, \bar{Y}, \bar{Z}$ axes, respectively. These displacements are shown graphically in Fig. 3.1.

Only small translations and rotations are considered. Hence, the rotations are commutative (i.e., the resulting position is independent of the order of the component rotations) and the angles of rotation about the body axes are equal to those about the inertial axes. Therefore, the displacements of a point b in the body (with the coordinates b_x, b_y, b_z in the X, Y, Z directions, respectively) are the sums of the components of the center-of-mass displacement in the directions of the $\bar{X}, \bar{Y}, \bar{Z}$ axes plus the tangential components of the rotational displacement of the body:

$$\begin{aligned} x_b &= x_c + b_z\beta - b_y\gamma \\ y_b &= y_c - b_z\alpha + b_x\gamma \\ z_b &= z_c - b_x\beta + b_y\alpha \end{aligned} \tag{3.1}$$

EQUATIONS OF SMALL MOTION OF A RIGID BODY

The equations of motion for the translation of a rigid body are

$$m\ddot{x}_c = \mathbf{F}_x \quad m\ddot{y}_c = \mathbf{F}_y \quad m\ddot{z}_c = \mathbf{F}_z \tag{3.2}$$

where m is the mass of the body, $\mathbf{F}_x, \mathbf{F}_y, \mathbf{F}_z$ are the summation of all forces acting on the body, and $\ddot{x}_c, \ddot{y}_c, \ddot{z}_c$ are the accelerations of the center-of-mass of the body in the $\bar{X}, \bar{Y}, \bar{Z}$ directions, respectively. The motion of the center-of-mass of a rigid body is the same as the motion of a particle having a mass equal to the total mass of the body and acted upon by the resultant external force.

The equations of motion for the rotation of a rigid body are

$$\begin{aligned} I_{xx}\ddot{\alpha} - I_{xy}\ddot{\beta} - I_{xz}\ddot{\gamma} &= \mathbf{M}_x \\ -I_{xy}\ddot{\alpha} + I_{yy}\ddot{\beta} - I_{yz}\ddot{\gamma} &= \mathbf{M}_y \\ -I_{xz}\ddot{\alpha} - I_{yz}\ddot{\beta} + I_{zz}\ddot{\gamma} &= \mathbf{M}_z \end{aligned} \tag{3.3}$$

where $\ddot{\alpha}$, $\ddot{\beta}$, $\ddot{\gamma}$ are the rotational accelerations about the X , Y , Z axes, as shown in Fig. 3.1; \mathbf{M}_x , \mathbf{M}_y , \mathbf{M}_z are the summation of torques acting on the rigid body about the axes X , Y , Z , respectively; and $I_{xx} \dots$, $I_{xy} \dots$ are the moments and products of inertia of the rigid body as defined below.

INERTIAL PROPERTIES OF A RIGID BODY

The properties of a rigid body that are significant in dynamics and vibration are the mass, the position of the center-of-mass (or center-of-gravity), the moments of inertia, the products of inertia, and the directions of the principal inertial axes. This section discusses the properties of a rigid body, together with computational and experimental methods for determining the properties.

MASS

Computation of Mass. The mass of a body is computed by integrating the product of mass density $\rho(V)$ and elemental volume dV over the body:

$$m = \int_V \rho(V) dV \quad (3.4)$$

If the body is made up of a number of elements, each having constant or an average density, the mass is

$$m = \rho_1 V_1 + \rho_2 V_2 + \dots + \rho_n V_n \quad (3.5)$$

where ρ_1 is the density of the element V_1 , etc. Densities of various materials may be found in handbooks containing properties of materials.¹

If a rigid body has a common geometrical shape, or if it is an assembly of sub-bodies having common geometrical shapes, the volume may be found from compilations of formulas. Typical formulas are included in Tables 3.1 and 3.2. Tables of areas of plane sections as well as volumes of solid bodies are useful.

If the volume of an element of the body is not given in such a table, the integration of Eq. (3.4) may be carried out analytically, graphically, or numerically. A graphical approach may be used if the shape is so complicated that the analytical expression for its boundaries is not available or is not readily integrable. This is accomplished by graphically dividing the body into smaller parts, each of whose boundaries may be altered slightly (without change to the area) in such a manner that the volume is readily calculable or measurable.

The weight W of a body of mass m is a function of the acceleration of gravity g at the particular location of the body in space:

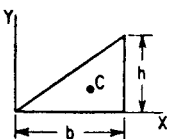
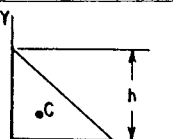
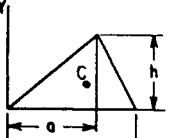
$$W = mg \quad (3.6)$$

Unless otherwise stated, it is understood that the weight of a body is given for an average value of the acceleration of gravity on the surface of the earth. For engineering purposes, $g = 32.2 \text{ ft/sec}^2$ or 386 in./sec^2 (9.81 m/sec^2) is usually used.

Experimental Determination of Mass. Although Newton's second law of motion, $F = m\ddot{x}$, may be used to measure mass, this usually is not convenient. The mass of a body is most easily measured by performing a static measurement of the weight of the body and converting the result to mass. This is done by use of the value of the acceleration of gravity at the measurement location [Eq. (3.6)].

TABLE 3.1 Properties of Plane Sections (After G. W. Housner and D. E. Hudson.²)

The dimensions X_c , Y_c are the X , Y coordinates of the centroid, A is the area, $I_x \dots$ is the area moment of inertia with respect to the $X \dots$ axis, $\rho_x \dots$ is the radius of gyration with respect to the $X \dots$ axis; uniform solid cylindrical bodies of length l in the Z direction having the various plane sections as their cross sections have mass moment and product of inertia values about the Z axis equal to ρl times the values given in the table, where ρ is the mass density of the body; the radii of gyration are unchanged.

Plane section	Area and centroid	Area moment of inertia	Square of radius of gyration	Area product of inertia
<p>1</p>  <p>Right triangle</p>	$A = \frac{1}{2}bh$ $X_c = \frac{2}{3}b$ $Y_c = \frac{1}{3}h$	$I_{x_c} = \frac{bh^3}{36}$ $I_{y_c} = \frac{b^3h}{36}$	$\rho_{x_c}^2 = \frac{1}{18}h^2$ $\rho_{y_c}^2 = \frac{1}{18}b^2$	$I_{x_c y_c} = \frac{A}{36}hb = \frac{h^2b^2}{72}$
<p>2</p> 	$A = \frac{1}{2}bh$ $X_c = \frac{1}{3}b$ $Y_c = \frac{2}{3}h$	$I_{x_c} = \frac{bh^3}{36}$ $I_{y_c} = \frac{b^3h}{36}$	$\rho_{x_c}^2 = \frac{1}{18}h^2$ $\rho_{y_c}^2 = \frac{1}{18}b^2$	$I_{x_c y_c} = -\frac{A}{36}hb = -\frac{h^2b^2}{72}$
<p>3</p>  <p>Triangle</p>	$A = \frac{1}{2}bh$ $X_c = \frac{1}{3}(a + b)$ $Y_c = \frac{1}{3}h$	$I_{x_c} = \frac{bh^3}{36}$ $I_{y_c} = \frac{bh}{36}(b^2 - ab + a^2)$	$\rho_{x_c}^2 = \frac{1}{18}A^2$ $\rho_{y_c}^2 = \frac{1}{18}(b^2 - ab + a^2)$	$I_{x_c y_c} = \frac{Ah}{36}(2a - b) = \frac{bh^2}{72}(2a - b)$

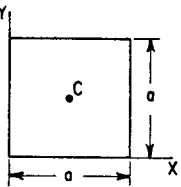
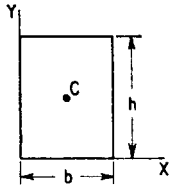
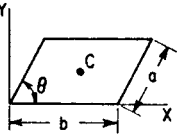
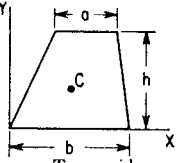
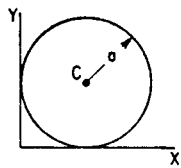
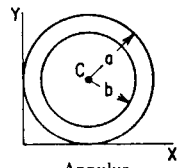
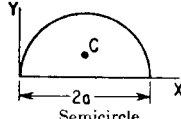
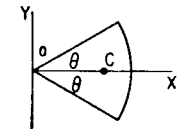
<p>4</p>  <p>Square</p>	$A = a^2$ $X_c = \frac{1}{2}a$ $Y_c = \frac{1}{2}a$	$I_{x_c} = I_{y_c} = \frac{a^4}{12}$	$\rho_{x_c^2} = \rho_{y_c^2} = \frac{1}{12}a^2$	$I_{x_c y_c} = 0$
<p>5</p>  <p>Rectangle</p>	$A = bh$ $X_c = \frac{1}{2}b$ $Y_c = \frac{1}{2}h$	$I_{x_c} = \frac{bh^3}{12}$ $I_{y_c} = \frac{b^3h}{12}$	$\rho_{x_c^2} = \frac{1}{12}h^2$ $\rho_{y_c^2} = \frac{1}{12}b^2$	$I_{x_c y_c} = 0$
<p>6</p>  <p>Parallelogram</p>	$A = ab \sin \theta$ $X_c = \frac{1}{2}(b + a \cos \theta)$ $Y_c = \frac{1}{2}(a \sin \theta)$	$I_{x_c} = \frac{a^3 b}{12} \sin^2 \theta$ $I_{y_c} = \frac{ab}{12} \sin \theta (b^2 + a^2 \cos^2 \theta)$	$\rho_{x_c^2} = \frac{1}{12}(a \sin \theta)^2$ $\rho_{y_c^2} = \frac{1}{12}(b^2 + a^2 \cos^2 \theta)$	$I_{x_c y_c} = \frac{a^3 b}{12} \sin^2 \theta \cos \theta$
<p>7</p>  <p>Trapezoid</p>	$A = \frac{1}{2}h(a + b)$ $Y_c = \frac{1}{6}h \left(\frac{2a + b}{a + b} \right)$	$I_{x_c} = \frac{h^3(a^2 + 4ab + b^2)}{36(a + b)}$	$\rho_{x_c^2} = \frac{h^2(a^2 + 4ab + b^2)}{18(a + b)^2}$	

TABLE 3.1 Properties of Plane Sections (Continued)

Plane Section	Area and centroid	Area moment of inertia	Square of radius of gyration	Area product of inertia
<p>8</p>  <p>Circle</p>	$A = \pi a^2$ $X_c = a$ $Y_c = a$	$I_{x_c} = I_{y_c} = \frac{1}{4}\pi a^4$	$\rho_{x_c}^2 = \rho_{y_c}^2 = \frac{1}{4}a^2$	$I_{x_c y_c} = 0$
<p>9</p>  <p>Annulus</p>	$A = \pi(a^2 - b^2)$ $X_c = a$ $Y_c = a$	$I_{x_c} = I_{y_c} = \frac{\pi}{4}(a^4 - b^4)$	$\rho_{x_c}^2 = \rho_{y_c}^2 = \frac{1}{4}(a^2 + b^2)$	$I_{x_c y_c} = 0$
<p>10</p>  <p>Semicircle</p>	$A = \frac{1}{2}\pi a^2$ $X_c = a$ $Y_c = \frac{4a}{3\pi}$	$I_{x_c} = \frac{a^4(9\pi^2 - 64)}{72\pi}$ $I_{y_c} = \frac{1}{8}\pi a^4$	$\rho_{x_c}^2 = \frac{a^2(9\pi^2 - 64)}{36\pi^2}$ $\rho_{y_c}^2 = \frac{1}{4}a^2$	$I_{x_c y_c} = 0$
<p>11</p>  <p>Circular sector</p>	$A = a^2\theta$ $X_c = \frac{2a}{3} \frac{\sin \theta}{\theta}$ $Y_c = 0$	$I_x = \frac{1}{4}a^4(\theta - \sin \theta \cos \theta)$ $I_y = \frac{1}{4}a^4(\theta + \sin \theta \cos \theta)$	$\rho_x^2 = \frac{1}{4}a^2 \left(\frac{\theta - \sin \theta \cos \theta}{\theta} \right)$ $\rho_y^2 = \frac{1}{4}a^2 \left(\frac{\theta + \sin \theta \cos \theta}{\theta} \right)$	$I_{x_c y_c} = 0$ $I_{xy} = 0$

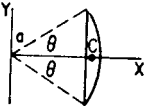
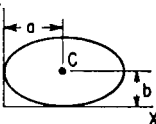
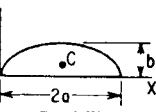
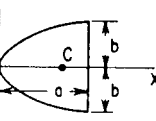
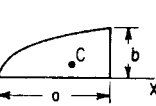
<p>12</p>  <p>Circular segment</p>	$A = a^2(\theta - \frac{1}{2} \sin 2\theta)$ $X_c = \frac{2a}{3} \left(\frac{\sin^3 \theta}{\theta - \sin \theta \cos \theta} \right)$ $Y_c = 0$	$I_x = \frac{Aa^2}{4} \left[1 - \frac{2 \sin^3 \theta \cos \theta}{3(\theta - \sin \theta \cos \theta)} \right]$ $I_y = \frac{Aa^2}{4} \left[1 + \frac{2 \sin^3 \theta \cos \theta}{\theta - \sin \theta \cos \theta} \right]$	$\rho_x^2 = \frac{a^2}{4} \left[1 - \frac{2 \sin^3 \theta \cos \theta}{3(\theta - \sin \theta \cos \theta)} \right]$ $\rho_y^2 = \frac{a^2}{4} \left[1 + \frac{2 \sin^3 \theta \cos \theta}{\theta - \sin \theta \cos \theta} \right]$	$I_{x_c y_c} = 0$ $I_{xy} = 0$
<p>13</p>  <p>Ellipse</p>	$A = \pi ab$ $X_c = a$ $Y_c = b$	$I_{x_c} = \frac{\pi}{4} ab^3$ $I_{y_c} = \frac{\pi}{4} a^3 b$	$\rho_{x_c}^2 = \frac{1}{4} b^2$ $\rho_{y_c}^2 = \frac{1}{4} a^2$	$I_{x_c y_c} = 0$
<p>14</p>  <p>Semiellipse</p>	$A = \frac{1}{2} \pi ab$ $X_c = a$ $Y_c = \frac{4b}{3\pi}$	$I_{x_c} = \frac{ab^3}{72\pi} (9\pi^2 - 64)$ $I_{y_c} = \frac{\pi}{8} a^3 b$	$\rho_{x_c}^2 = \frac{b^2}{36\pi^2} (9\pi^2 - 64)$ $\rho_{y_c}^2 = \frac{1}{4} a^2$	$I_{x_c y_c} = 0$
<p>15</p>  <p>Parabola</p>	$A = \frac{2}{3} ab$ $X_c = \frac{3}{8} a$ $Y_c = 0$	$I_{x_c} = \frac{1}{4} sab^3$ $I_{y_c} = \frac{1}{4} (7sa^3)b$	$\rho_{x_c}^2 = \frac{1}{4} b^2$ $\rho_{y_c}^2 = \frac{1}{4} (7sa^2)$	$I_{x_c y_c} = 0$
<p>16</p>  <p>Semiparabola</p>	$A = \frac{3}{8} ab$ $X_c = \frac{3}{8} a$ $Y_c = \frac{3}{16} b$	$I_x = \frac{3}{4} sab^3$ $I_y = \frac{3}{4} a^3 b$	$\rho_x^2 = \frac{1}{4} b^2$ $\rho_y^2 = \frac{3}{4} a^2$	$I_{xy} = \frac{A}{4} ab = \frac{1}{64} a^2 b^2$

TABLE 3.1 Properties of Plane Sections (*Continued*)

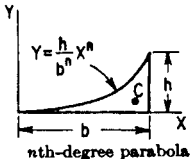
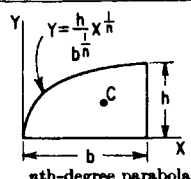
Plane section	Area and centroid	Area moment of inertia	Square of radius of gyration	Area product of inertia
17  <p>$Y = \frac{h}{b^n} X^n$</p> <p>nth-degree parabola</p>	$A = \frac{bh}{n+1}$ $X_c = \frac{n+1}{n+2} b$ $Y_c = \frac{h}{2} \left(\frac{n+1}{2n+1} \right)$	$I_x = \frac{bh^3}{3(3n+1)}$ $I_y = \frac{hb^3}{n+3}$	$\rho_x^2 = \frac{h^2(n+1)}{3(3n+1)}$ $\rho_y^2 = \frac{n+1}{n+3} b^2$	
18  <p>$Y = \frac{h}{b^n} X^{n+1}$</p> <p>nth-degree parabola</p>	$A = \frac{n}{n+1} bh$ $X_c = \frac{n+1}{2n+1} b$ $Y_c = \frac{n+1}{2(n+2)} h$	$I_x = \frac{n}{3(n+3)} bh^3$ $I_y = \frac{n}{3n+1} hb^3$	$\rho_x^2 = \frac{n+1}{3(n+3)} h^2$ $\rho_y^2 = \frac{n+1}{3n+1} b^2$	

TABLE 3.2 Properties of Homogeneous Solid Bodies (After G. W. Housner and D. E. Hudson.²)

The dimensions X_c, Y_c, Z_c are the X, Y, Z coordinates of the centroid, S is the cross-sectional area of the thin rod or hoop in cases 1 to 3, V is the volume, $I_x \dots$ is the mass moment of inertia with respect to the $X \dots$ axis, $\rho_x \dots$ is the radius of gyration with respect to the $X \dots$ axis, ρ is the mass density of the body.

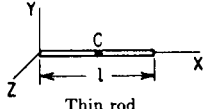
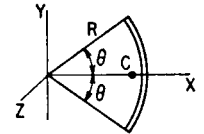
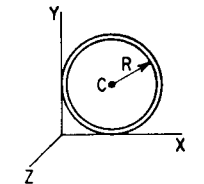
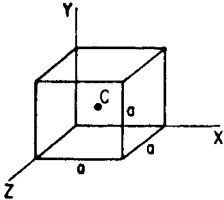
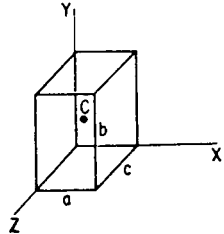
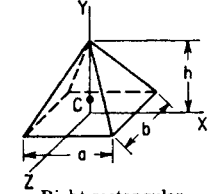
Solid body	Volume and centroid	Mass moment of inertia	Radius of gyration squared	Mass product of inertia
<p>1</p>  <p>Thin rod</p>	$V = Sl$ $X_c = \frac{1}{2}l$ $Y_c = 0$ $Z_c = 0$	$I_{x_c} = 0$ $I_{y_c} = I_{z_c} = \frac{\rho V}{12} l^2$	$\rho_{x_c}^2 = 0$ $\rho_{y_c}^2 = \rho_{z_c}^2 = \frac{1}{12} l^2$	$I_{x_c y_c}, \text{ etc.} = 0$
<p>2</p>  <p>Thin circular rod</p>	$V = 2SR\theta$ $X_c = \frac{R \sin \theta}{\theta}$ $Y_c = 0$ $Z_c = 0$	$I_x = I_{x_c}$ $= \frac{\rho V R^2 (\theta - \sin \theta \cos \theta)}{2\theta}$ $I_y = \frac{\rho V R^2 (\theta + \sin \theta \cos \theta)}{2\theta}$ $I_z = \rho V R^2$	$\rho_x^2 = \rho_{x_c}^2 = \frac{R^2 (\theta - \sin \theta \cos \theta)}{2\theta}$ $r_y^2 = \frac{R^2 (\theta + \sin \theta \cos \theta)}{2\theta}$ $\rho_z^2 = R^2$	$I_{x_c y_c}, \text{ etc.} = 0$ $I_{x y}, \text{ etc.} = 0$
<p>3</p> 	$V = 2\pi SR$ $X_c = R$ $Y_c = R$ $Z_c = 0$	$I_{x_c} = I_{y_c} = \frac{\rho V}{2} R^2$ $I_{z_c} = \rho V R^2$	$\rho_{x_c}^2 = \rho_{y_c}^2 = \frac{1}{2} R^2$ $\rho_{z_c}^2 = R^2$	$I_{x_c y_c}, \text{ etc.} = 0$

TABLE 3.2 Properties of Homogeneous Solid Bodies (Continued)

Solid body	Volume and centroid	Mass moment of inertia	Radius of gyration squared	Mass product of inertia
<p>4</p>  <p>Cube</p>	$V = a^3$ $X_c = \frac{1}{2}a$ $Y_c = \frac{1}{2}a$ $Z_c = \frac{1}{2}a$	$I_{x_c} = I_{y_c} = I_{z_c} = \frac{1}{6}\rho Va^2$	$\rho x_c^2 = \rho y_c^2 = \rho z_c^2 = \frac{1}{6}a^2$	$I_{x_c y_c}, \text{ etc.} = 0$
<p>5</p>  <p>Rectangular prism</p>	$V = abc$ $X_c = \frac{1}{2}a$ $Y_c = \frac{1}{2}b$ $Z_c = \frac{1}{2}c$	$I_{x_c} = \frac{1}{12}\rho V(b^2 + c^2)$	$\rho x_c^2 = \frac{1}{12}(b^2 + c^2)$	$I_{x_c y_c}, \text{ etc.} = 0$
<p>6</p>  <p>Right rectangular pyramid</p>	$V = \frac{1}{3}abh$ $X_c = 0$ $Y_c = \frac{1}{4}h$ $Z_c = 0$	$I_{x_c} = \frac{1}{80}\rho V(4b^2 + 3h^2)$ $I_{y_c} = \frac{1}{80}\rho V(a^2 + b^2)$	$\rho x_c^2 = \frac{1}{80}(4b^2 + 3h^2)$ $\rho y_c^2 = \frac{1}{80}(a^2 + b^2)$	$I_{x_c y_c}, \text{ etc.} = 0$

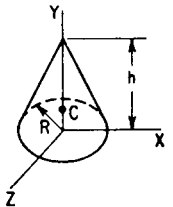
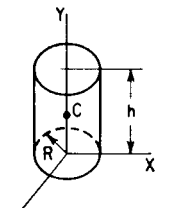
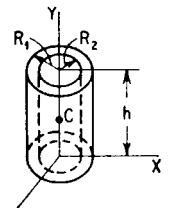
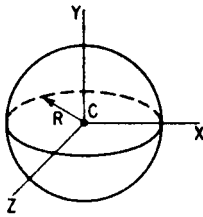
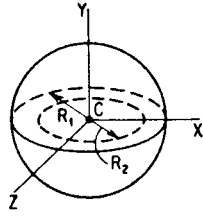
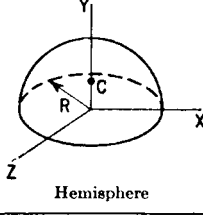
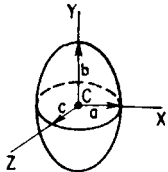
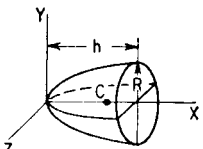
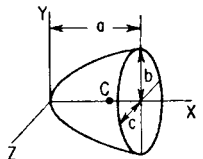
<p>7</p>  <p>Right circular cone</p>	$V = \frac{1}{3}\pi R^2 h$ $X_c = 0$ $Y_c = \frac{1}{4}h$ $Z_c = 0$	$I_{x_c} = I_{y_c} = \frac{3\rho V}{80} (4R^2 + h^2)$ $I_{z_c} = \frac{3}{10}\rho V R^2$	$\rho_{x_c}^2 = \rho_{y_c}^2 = \frac{3}{80}(4R^2 + h^2)$ $\rho_{z_c}^2 = \frac{3}{10}R^2$	$I_{x_c y_c}, \text{ etc.} = 0$
<p>8</p>  <p>Right circular cylinder</p>	$V = \pi R^2 h$ $X_c = 0$ $Y_c = \frac{1}{2}h$ $Z_c = 0$	$I_{x_c} = I_{y_c} = \frac{1}{12}\rho V (3R^2 + h^2)$ $I_{z_c} = \frac{1}{2}\rho V R^2$	$\rho_{x_c}^2 = \rho_{y_c}^2 = \frac{1}{12}(3R^2 + h^2)$ $\rho_{z_c}^2 = \frac{1}{2}R^2$	$I_{x_c y_c}, \text{ etc.} = 0$
<p>9</p>  <p>Hollow right circular cylinder</p>	$V = \pi h (R_1^2 - R_2^2)$ $X_c = 0$ $Y_c = \frac{1}{2}h$ $Z_c = 0$	$I_{x_c} = I_{y_c}$ $= \frac{1}{12}\rho V (3R_1^2 + 3R_2^2 + h^2)$ $I_{z_c} = \frac{1}{2}\rho V (R_1^2 + R_2^2)$	$\rho_{x_c}^2 = \rho_{y_c}^2 = \frac{1}{12}(3R_1^2 + 3R_2^2 + h^2)$ $\rho_{z_c}^2 = \frac{1}{2}(R_1^2 + R_2^2)$	$I_{x_c y_c}, \text{ etc.} = 0$

TABLE 3.2 Properties of Homogeneous Solid Bodies (Continued)

Solid body	Volume and centroid	Mass moment of inertia	Radius of gyration squared	Mass product of inertia
<p>10</p>  <p>Sphere</p>	$V = \frac{4}{3}\pi R^3$ $X_c = 0$ $Y_c = 0$ $Z_c = 0$	$I_{x_c} = \frac{3}{2}\rho V R^2$ $I_{y_c} = \frac{3}{2}\rho V R^2$ $I_{z_c} = \frac{3}{2}\rho V R^2$	$\rho x_c^2 = \frac{3}{2}R^2$ $\rho y_c^2 = \frac{3}{2}R^2$ $\rho z_c^2 = \frac{3}{2}R^2$	$I_{x_c y_c}, \text{ etc.} = 0$
<p>11</p>  <p>Hollow sphere</p>	$V = \frac{4}{3}\pi(R_1^3 - R_2^3)$ $X_c = 0$ $Y_c = 0$ $Z_c = 0$	$I_x = I_y = I_z$ $= \frac{2}{5} \rho V \frac{R_1^5 - R_2^5}{R_1^3 - R_2^3}$	$\rho x^2 = \rho y^2 = \rho z^2$ $= \frac{2}{5} \frac{R_1^6 - R_2^6}{R_1^3 - R_2^3}$	$I_{xy}, \text{ etc.} = 0$
<p>12</p>  <p>Hemisphere</p>	$V = \frac{2}{3}\pi R^3$ $X_c = 0$ $Y_c = \frac{3}{8}R$ $Z_c = 0$	$I_x = I_y = I_z = \frac{3}{2}\rho V R^2$	$\rho x^2 = \rho y^2 = \rho z^2 = \frac{3}{2}R^2$	$I_{x_c y_c}, \text{ etc.} = 0$ $I_{xy}, \text{ etc.} = 0$

<p>13</p>  <p>Ellipsoid</p>	$V = \frac{4}{3}\pi abc$ $X_c = 0$ $Y_c = 0$ $Z_c = 0$	$I_x = \frac{1}{60}\rho V(b^2 + c^2)$ $I_y = \frac{1}{60}\rho V(a^2 + c^2)$ $I_z = \frac{1}{60}\rho V(a^2 + b^2)$	$\rho_x^2 = \frac{1}{6}(b^2 + c^2)$ $\rho_y^2 = \frac{1}{6}(a^2 + c^2)$ $\rho_z^2 = \frac{1}{6}(a^2 + b^2)$	$I_{xy}, \text{ etc.} = 0$
<p>14</p>  <p>Paraboloid of revolution</p>	$V = \frac{1}{2}\pi R^2 h$ $X_c = \frac{3}{8}h$ $Y_c = 0$ $Z_c = 0$	$I_{x_c} = \frac{1}{60}\rho V R^2$ $I_{y_c} = I_{z_c} = \frac{1}{18}\rho V(3R^2 + h^2)$	$\rho_{x_c}^2 = \frac{1}{8}R^2$ $\rho_{y_c}^2 = \rho_{z_c}^2 = \frac{1}{18}(3R^2 + h^2)$	$I_{x_c y_c}, \text{ etc.} = 0$
<p>15</p>  <p>Elliptic paraboloid</p>	$V = \frac{1}{2}\pi abc$ $X_c = \frac{3}{8}a$ $Y_c = 0$ $Z_c = 0$	$I_{x_c} = \frac{1}{60}\rho V(b^2 + c^2)$ $I_{y_c} = \frac{1}{18}\rho V(3c^2 + a^2)$ $I_{z_c} = \frac{1}{18}\rho V(3b^2 + a^2)$	$\rho_{x_c}^2 = \frac{1}{6}(b^2 + c^2)$ $\rho_{y_c}^2 = \frac{1}{18}(3c^2 + a^2)$ $\rho_{z_c}^2 = \frac{1}{18}(3b^2 + a^2)$	$I_{x_c y_c}, \text{ etc.} = 0$

CENTER-OF-MASS

Computation of Center-of-Mass. The center-of-mass (or center-of-gravity) is that point located by the vector

$$\mathbf{r}_c = \frac{1}{m} \int_m \mathbf{r}(m) dm \quad (3.7)$$

where $\mathbf{r}(m)$ is the radius vector of the element of mass dm . The center-of-mass of a body in a cartesian coordinate system X, Y, Z is located at

$$\begin{aligned} X_c &= \frac{1}{m} \int_V X(V) \rho(V) dV \\ Y_c &= \frac{1}{m} \int_V Y(V) \rho(V) dV \\ Z_c &= \frac{1}{m} \int_V Z(V) \rho(V) dV \end{aligned} \quad (3.8)$$

where $X(V), Y(V), Z(V)$ are the X, Y, Z coordinates of the element of volume dV and m is the mass of the body.

If the body can be divided into elements whose centers-of-mass are known, the center-of-mass of the entire body having a mass m is located by equations of the following type:

$$X_c = \frac{1}{m} (X_{c1}m_1 + X_{c2}m_2 + \dots + X_{cn}m_n), \text{ etc.} \quad (3.9)$$

where X_{c1} is the X coordinate of the center-of-mass of element m_1 . Tables (see Tables 3.1 and 3.2) which specify the location of centers of area and volume (called centroids) for simple sections and solid bodies often are an aid in dividing the body into the submasses indicated in the above equation. The centroid and center-of-mass of an element are coincident when the density of the material is uniform throughout the element.

Experimental Determination of Center-of-Mass. The location of the center-of-mass is normally measured indirectly by locating the center-of-gravity of the body, and may be found in various ways. Theoretically, if the body is suspended by a flexible wire attached successively at different points on the body, all lines represented by the wire in its various positions when extended inwardly into the body intersect at the center-of-gravity. Two such lines determine the center-of-gravity, but more may be used as a check. There are practical limitations to this method in that the point of intersection often is difficult to designate.

Other techniques are based on the balancing of the body on point or line supports. A point support locates the center-of-gravity along a vertical line through the point; a line support locates it in a vertical plane through the line. The intersection of such lines or planes determined with the body in various positions locates the center-of-gravity. The greatest difficulty with this technique is the maintenance of the stability of the

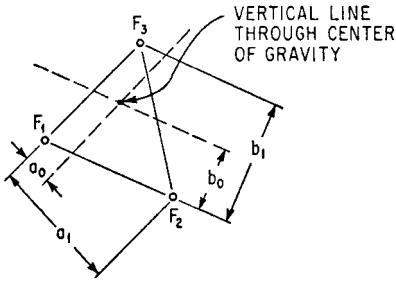


FIGURE 3.2 Three-scale method of locating the center-of-gravity of a body. The vertical forces F_1, F_2, F_3 at the scales result from the weight of the body. The vertical line located by the distances a_0 and b_0 [see Eqs. (3.10)] passes through the center-of-gravity of the body.

body while it is balanced, particularly where the height of the body is great relative to a horizontal dimension. If a perfect point or edge support is used, the equilibrium position is inherently unstable. It is only if the support has width that some degree of stability can be achieved, but then a resulting error in the location of the line or plane containing the center-of-gravity can be expected.

Another method of locating the center-of-gravity is to place the body in a stable position on three scales. From static moments the vector weight of the body is the resultant of the measured forces at the scales, as shown in Fig. 3.2. The vertical line through the center-of-gravity is located by the distances a_0 and b_0 :

$$a_0 = \frac{F_2}{F_1 + F_2 + F_3} a_1$$

$$b_0 = \frac{F_3}{F_1 + F_2 + F_3} b_1$$
(3.10)

This method cannot be used with more than three scales.

MOMENT AND PRODUCT OF INERTIA

Computation of Moment and Product of Inertia^{2,3} The moments of inertia of a rigid body with respect to the orthogonal axes X, Y, Z fixed in the body are

$$I_{xx} = \int_m (Y^2 + Z^2) dm \quad I_{yy} = \int_m (X^2 + Z^2) dm \quad I_{zz} = \int_m (X^2 + Y^2) dm \quad (3.11)$$

where dm is the infinitesimal element of mass located at the coordinate distances X, Y, Z ; and the integration is taken over the mass of the body. Similarly, the products of inertia are

$$I_{xy} = \int_m XY dm \quad I_{xz} = \int_m XZ dm \quad I_{yz} = \int_m YZ dm \quad (3.12)$$

It is conventional in rigid body mechanics to take the center of coordinates at the center-of-mass of the body. Unless otherwise specified, this location is assumed, and the moments of inertia and products of inertia refer to axes through the center-of-mass of the body. For a unique set of axes, the products of inertia vanish. These axes are called the principal inertial axes of the body. The moments of inertia about these axes are called the principal moments of inertia. The moments of inertia of a rigid body can be defined in terms of radii of gyration as follows:

$$I_{xx} = m\rho_x^2 \quad I_{yy} = m\rho_y^2 \quad I_{zz} = m\rho_z^2 \quad (3.13)$$

where $I_{xx} \dots$ are the moments of inertia of the body as defined by Eqs. (3.11), m is the mass of the body, and $\rho_{xx} \dots$ are the radii of gyration. The radius of gyration has the dimension of length, and often leads to convenient expressions in dynamics of rigid bodies when distances are normalized to an appropriate radius of gyration. Solid bodies of various shapes have characteristic radii of gyration which sometimes are useful intuitively in evaluating dynamic conditions.

Unless the body has a very simple shape, it is laborious to evaluate the integrals of Eqs. (3.11) and (3.12). The problem is made easier by subdividing the body into parts for which simplified calculations are possible. The moments and products of inertia of the body are found by first determining the moments and products of inertia for the individual parts with respect to appropriate reference axes chosen in the parts, and then summing the contributions of the parts. This is done by selecting axes through the centers-of-mass of the parts, and then determining the moments and products of inertia of the parts relative to these axes. Then the moments and products of inertia are transferred to the axes chosen through the center-of-mass of the whole body, and the transferred quantities summed. In general, the transfer involves

two sets of nonparallel coordinates whose centers are displaced. Two transformations are required as follows.

Transformation to Parallel Axes.

Referring to Fig. 3.3, suppose that X, Y, Z is a convenient set of axes for the moment of inertia of the whole body with its origin at the center-of-mass. The moments and products of inertia for a part of the body are $I_{x''x''}, I_{y''y''}, I_{z''z''}, I_{x''y''}, I_{x''z''}$ and $I_{y''z''}$ taken with respect to a set of axes X'', Y'', Z'' fixed in the part and having their center at the center-of-mass of the part. The axes X', Y', Z' are chosen parallel to X'', Y'', Z'' with their origin at the center-of-mass of the body. The perpendicular distance between the X'' and X' axes is a_x ; that between Y'' and Y' is a_y ; that between Z'' and Z' is a_z . The moments and products of inertia of the part of mass m_n with respect to the X', Y', Z' axes are

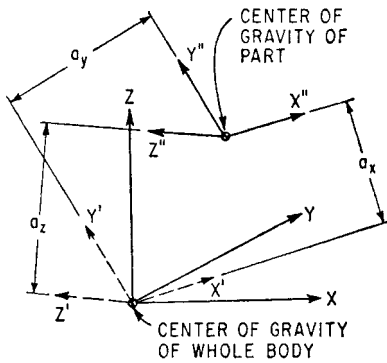


FIGURE 3.3 Axes required for moment and product of inertia transformations. Moments and products of inertia with respect to the axes X'', Y'', Z'' are transferred to the mutually parallel axes X', Y', Z' by Eqs. (3.14) and (3.15), and then to the inclined axes X, Y, Z by Eqs. (3.16) and (3.17).

$$\begin{aligned}
 I_{x'x'} &= I_{x''x''} + m_n a_x^2 \\
 I_{y'y'} &= I_{y''y''} + m_n a_y^2 \\
 I_{z'z'} &= I_{z''z''} + m_n a_z^2
 \end{aligned}
 \tag{3.14}$$

The corresponding products of inertia are

$$\begin{aligned}
 I_{x'y'} &= I_{x''y''} + m_n a_x a_y \\
 I_{x'z'} &= I_{x''z''} + m_n a_x a_z \\
 I_{y'z'} &= I_{y''z''} + m_n a_y a_z
 \end{aligned}
 \tag{3.15}$$

If X'', Y'', Z'' are the principal axes of the part, the product of inertia terms on the right-hand side of Eqs. (3.15) are zero.

Transformation to Inclined Axes. The desired moments and products of inertia with respect to axes X, Y, Z are now obtained by a transformation theorem relating the properties of bodies with respect to inclined sets of axes whose centers coincide. This theorem makes use of the direction cosines λ for the respective sets of axes. For example, $\lambda_{xx'}$ is the cosine of the angle between the X and X' axes. The expressions for the moments of inertia are

$$\begin{aligned}
 I_{xx} &= \lambda_{xx'}^2 I_{x'x'} + \lambda_{xy'}^2 I_{y'y'} + \lambda_{xz'}^2 I_{z'z'} - 2\lambda_{xx'}\lambda_{xy'} I_{x'y'} - 2\lambda_{xx'}\lambda_{xz'} I_{x'z'} - 2\lambda_{xy'}\lambda_{xz'} I_{y'z'} \\
 I_{yy} &= \lambda_{yx'}^2 I_{x'x'} + \lambda_{yy'}^2 I_{y'y'} + \lambda_{yz'}^2 I_{z'z'} - 2\lambda_{yx'}\lambda_{yy'} I_{x'y'} - 2\lambda_{yx'}\lambda_{yz'} I_{x'z'} - 2\lambda_{yy'}\lambda_{yz'} I_{y'z'} \\
 I_{zz} &= \lambda_{zx'}^2 I_{x'x'} + \lambda_{zy'}^2 I_{y'y'} + \lambda_{zz'}^2 I_{z'z'} - 2\lambda_{zx'}\lambda_{zy'} I_{x'y'} - 2\lambda_{zx'}\lambda_{zz'} I_{x'z'} - 2\lambda_{zy'}\lambda_{zz'} I_{y'z'}
 \end{aligned} \tag{3.16}$$

The corresponding products of inertia are

$$\begin{aligned}
 -I_{xy} &= \lambda_{xx'}\lambda_{yx'} I_{x'x'} + \lambda_{xy'}\lambda_{yy'} I_{y'y'} + \lambda_{xz'}\lambda_{yz'} I_{z'z'} - (\lambda_{xx'}\lambda_{yy'} + \lambda_{xy'}\lambda_{yx'}) I_{x'y'} \\
 &\quad - (\lambda_{xy'}\lambda_{yz'} + \lambda_{xz'}\lambda_{zy'}) I_{y'z'} - (\lambda_{xz'}\lambda_{yx'} + \lambda_{xx'}\lambda_{yz'}) I_{x'z'} \\
 -I_{xz} &= \lambda_{xx'}\lambda_{zx'} I_{x'x'} + \lambda_{xy'}\lambda_{zy'} I_{y'y'} + \lambda_{xz'}\lambda_{zz'} I_{z'z'} - (\lambda_{xx'}\lambda_{zy'} + \lambda_{xy'}\lambda_{zx'}) I_{x'y'} \\
 &\quad - (\lambda_{xy'}\lambda_{zz'} + \lambda_{xz'}\lambda_{zy'}) I_{y'z'} - (\lambda_{xx'}\lambda_{zz'} + \lambda_{xz'}\lambda_{zx'}) I_{x'z'} \\
 -I_{yz} &= \lambda_{yx'}\lambda_{zx'} I_{x'x'} + \lambda_{yy'}\lambda_{zy'} I_{y'y'} + \lambda_{yz'}\lambda_{zz'} I_{z'z'} - (\lambda_{yx'}\lambda_{zy'} + \lambda_{yy'}\lambda_{zx'}) I_{x'y'} \\
 &\quad - (\lambda_{yy'}\lambda_{zz'} + \lambda_{yz'}\lambda_{zy'}) I_{y'z'} - (\lambda_{yz'}\lambda_{zx'} + \lambda_{yx'}\lambda_{zz'}) I_{x'z'}
 \end{aligned} \tag{3.17}$$

Experimental Determination of Moments of Inertia. The moment of inertia of a body about a given axis may be found experimentally by suspending the body as a pendulum so that rotational oscillations about that axis can occur. The period of free oscillation is then measured, and is used with the geometry of the pendulum to calculate the moment of inertia.

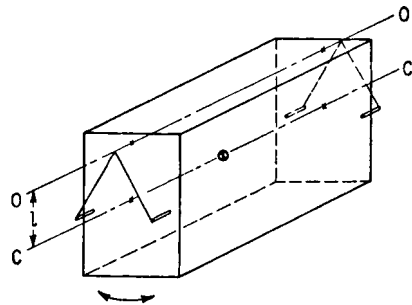


FIGURE 3.4 Compound pendulum method of determining moment of inertia. The period of oscillation of the test body about the horizontal axis $O-O$ and the perpendicular distance l between the axis $O-O$ and the parallel axis $C-C$ through the center-of-gravity of the test body give I_{cc} by Eq. (3.18).

Two types of pendulums are useful: the compound pendulum and the torsional pendulum. When using the compound pendulum, the body is supported from two overhead points by wires, illustrated in Fig. 3.4. The distance l is measured between the axis of support $O-O$ and a parallel axis $C-C$ through the center-of-gravity of the body. The moment of inertia about $C-C$ is given by

$$I_{cc} = ml^2 \left[\left(\frac{\tau_0}{2\pi} \right)^2 \left(\frac{g}{l} \right) - 1 \right] \tag{3.18}$$

where τ_0 is the period of oscillation in seconds, l is the pendulum length in inches, g is the gravitational acceleration in in./sec², and m is the mass in lb-sec²/in., yielding a moment of inertia in lb-in.-sec².

The accuracy of the above method is dependent upon the accuracy with which the distance l is known. Since the center-of-gravity often is an inaccessible point, a direct measurement of l may not be practicable. However, a change in l can be measured quite readily. If the experiment is repeated with a different support axis $O'-O'$, the length l becomes $l + \Delta l$ and the period of oscillation becomes τ'_0 . Then, the distance l can be written in terms of Δl and the two periods τ_0, τ'_0 :

$$l = \Delta l \left[\frac{(\tau_0'^2/4\pi^2)(g/\Delta l) - 1}{[(\tau_0^2 - \tau_0'^2)/4\pi^2][g/\Delta l] - 1} \right] \quad (3.19)$$

This value of l can be substituted into Eq. (3.18) to compute I_{cc} .

Note that accuracy is not achieved if l is much larger than the radius of gyration ρ_c of the body about the axis $C-C$ ($I_{cc} = m\rho_c^2$). If l is large, then $(\tau_0/2\pi)^2 \approx l/g$ and the expression in brackets in Eq. (3.18) is very small; thus, it is sensitive to small errors in the measurement of both τ_0 and l . Consequently, it is highly desirable that the distance l be chosen as small as convenient, preferably with the axis $O-O$ passing through the body.

A torsional pendulum may be constructed with the test body suspended by a single torsional spring (in practice, a rod or wire) of known stiffness, or by three flexible wires. A solid body supported by a single torsional spring is shown in Fig. 3.5. From the known torsional stiffness k_t and the measured period of torsional oscillation τ , the moment of inertia of the body about the vertical torsional axis is

$$I_{cc} = \frac{k_t \tau^2}{4\pi^2} \quad (3.20)$$

A platform may be constructed below the torsional spring to carry the bodies to be measured, as shown in Fig. 3.6. By repeating the experiment with two different bodies placed on the platform, it becomes unnecessary to measure the torsional stiffness k_t . If a body with a *known* moment of inertia I_1 is placed on the platform and an oscillation period τ_1 results, the moment of inertia I_2 of a body which produces a period τ_2 is given by

$$I_2 = I_1 \left[\frac{(\tau_2/\tau_0)^2 - 1}{(\tau_1/\tau_0)^2 - 1} \right] \quad (3.21)$$

where τ_0 is the period of the pendulum composed of platform alone.

A body suspended by three flexible wires, called a trifilar pendulum, as shown in Fig. 3.7, offers some utilitarian advantages. Designating the perpendicular distances

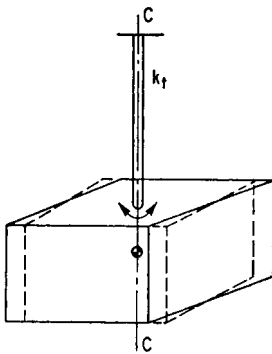


FIGURE 3.5 Torsional pendulum method of determining moment of inertia. The period of torsional oscillation of the test body about the vertical axis $C-C$ passing through the center-of-gravity and the torsional spring constant k_t give I_{cc} by Eq. (3.20).

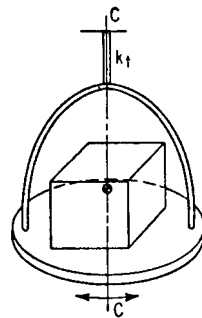


FIGURE 3.6 A variation of the torsional pendulum method shown in Fig. 3.5 wherein a light platform is used to carry the test body. The moment of inertia I_{cc} is given by Eq. (3.20).

of the wires to the vertical axis $C-C$ through the center-of-gravity of the body by R_1, R_2, R_3 , the angles between wires by ϕ_1, ϕ_2, ϕ_3 , and the length of each wire by l , the moment of inertia about axis $C-C$ is

$$I_{cc} = \frac{mgR_1R_2R_3\tau^2}{4\pi^2l} \frac{R_1 \sin \phi_1 + R_2 \sin \phi_2 + R_3 \sin \phi_3}{R_2R_3 \sin \phi_1 + R_1R_3 \sin \phi_2 + R_1R_2 \sin \phi_3} \quad (3.22)$$

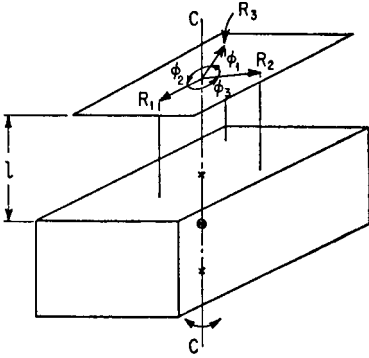


FIGURE 3.7 Trifilar pendulum method of determining moment of inertia. The period of torsional oscillation of the test body about the vertical axis $C-C$ passing through the center-of-gravity and the geometry of the pendulum give I_{cc} by Eq. (3.22); with a simpler geometry, I_{cc} is given by Eq. (3.23).

Apparatus that is more convenient for repeated use embodies a light platform supported by three equally spaced wires. The body whose moment of inertia is to be measured is placed on the platform with its center-of-gravity equidistant from the wires. Thus $R_1 = R_2 = R_3 = R$ and $\phi_1 = \phi_2 = \phi_3 = 120^\circ$. Substituting these relations in Eq. (3.22), the moment of inertia about the vertical axis $C-C$ is

$$I_{cc} = \frac{mgR^2\tau^2}{4\pi^2l} \quad (3.23)$$

where the mass m is the sum of the masses of the test body and the platform. The moment of inertia of the platform is subtracted from the test result to obtain the moment of inertia of the body being measured. It becomes unnecessary to know the distances R and l in Eq. (3.23) if the period of oscillation is measured with the platform empty, with

the body being measured on the platform, and with a second body of known mass m_1 and known moment of inertia I_1 on the platform. Then the desired moment of inertia I_2 is

$$I_2 = I_1 \left[\frac{[1 + (m_2/m_0)][\tau_2/\tau_0]^2 - 1}{[1 + (m_1/m_0)][\tau_1/\tau_0]^2 - 1} \right] \quad (3.24)$$

where m_0 is the mass of the unloaded platform, m_2 is the mass of the body being measured, τ_0 is the period of oscillation with the platform unloaded, τ_1 is the period when loaded with known body of mass m_1 , and τ_2 is the period when loaded with the unknown body of mass m_2 .

Experimental Determination of Product of Inertia. The experimental determination of a product of inertia usually requires the measurement of moments of inertia. (An exception is the balancing machine technique described later.) If possible, symmetry of the body is used to locate directions of principal inertial axes, thereby simplifying the relationship between the moments of inertia as known and the products of inertia to be found. Several alternative procedures are described below, depending on the number of principal inertia axes whose directions are known. Knowledge of two principal axes implies a knowledge of all three since they are mutually perpendicular.

If the directions of all three principal axes (X', Y', Z') are known and it is desirable to use another set of axes (X, Y, Z), Eqs. (3.16) and (3.17) may be simplified

because the products of inertia with respect to the principal directions are zero. First, the three principal moments of inertia ($I_{x'x'}$, $I_{y'y'}$, $I_{z'z'}$) are measured by one of the above techniques; then the moments of inertia with respect to the X, Y, Z axes are

$$\begin{aligned} I_{xx} &= \lambda_{xx}^2 I_{x'x'} + \lambda_{xy}^2 I_{y'y'} + \lambda_{xz}^2 I_{z'z'} \\ I_{yy} &= \lambda_{yx}^2 I_{x'x'} + \lambda_{yy}^2 I_{y'y'} + \lambda_{yz}^2 I_{z'z'} \\ I_{zz} &= \lambda_{zx}^2 I_{x'x'} + \lambda_{zy}^2 I_{y'y'} + \lambda_{zz}^2 I_{z'z'} \end{aligned} \tag{3.25}$$

The products of inertia with respect to the X, Y, Z axes are

$$\begin{aligned} -I_{xy} &= \lambda_{xx} \lambda_{yx} I_{x'x'} + \lambda_{xy} \lambda_{yy} I_{y'y'} + \lambda_{xz} \lambda_{yz} I_{z'z'} \\ -I_{xz} &= \lambda_{xx} \lambda_{zx} I_{x'x'} + \lambda_{xy} \lambda_{zy} I_{y'y'} + \lambda_{xz} \lambda_{zz} I_{z'z'} \\ -I_{yz} &= \lambda_{yx} \lambda_{zx} I_{x'x'} + \lambda_{yy} \lambda_{zy} I_{y'y'} + \lambda_{yz} \lambda_{zz} I_{z'z'} \end{aligned} \tag{3.26}$$

The direction of one principal axis Z may be known from symmetry. The axis through the center-of-gravity perpendicular to the plane of symmetry is a principal axis. The product of inertia with respect to X and Y axes, located in the plane of symmetry, is determined by first establishing another axis X' at a counterclockwise angle θ from X , as shown in Fig. 3.8. If the three moments of inertia I_{xx} , $I_{x'x'}$, and I_{yy} are measured by any applicable means, the product of inertia I_{xy} is

$$I_{xy} = \frac{I_{xx} \cos^2 \theta + I_{yy} \sin^2 \theta - I_{x'x'}}{\sin 2\theta} \tag{3.27}$$

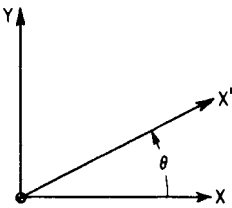


FIGURE 3.8 Axes required for determining the product of inertia with respect to the axes X and Y when Z is a principal axis of inertia. The moments of inertia about the axes X, Y , and X' , where X' is in the plane of X and Y at a counterclockwise angle θ from X , give I_{xy} by Eq. (3.27).

where $0 < \theta < \pi$. For optimum accuracy, θ should be approximately $\pi/4$ or $3\pi/4$. Since the third axis Z is a principal axis, I_{xz} and I_{yz} are zero.

Another method is illustrated in Fig. 3.9.^{4,5} The plane of the X and Z axes is a plane of symmetry, or the Y axis is otherwise known to be a principal axis of inertia. For determining I_{xz} , the body is suspended by a cable so that the Y axis is horizontal and the Z axis is vertical. Torsional stiffness about the Z axis is provided by four springs acting in the Y direction at the points shown. The body is oscillated about the Z axis with various positions of the springs so that the angle θ can be varied. The spring stiffnesses and locations must be such that there is no net force in the Y direction due to a rotation about the Z axis. In general, there is coupling between rotations about the X and Z axes, with the result that oscillations about both axes occur as a result of an initial rotational displacement about the Z axis. At some particular value of $\theta = \theta_0$, the two rotations are uncoupled; i.e., oscillation about the Z axis does not cause oscillation about the X axis. Then

$$I_{xz} = I_{zz} \tan \theta_0 \tag{3.28}$$

The moment of inertia I_{zz} can be determined by one of the methods described under *Experimental Determination of Moments of Inertia*.

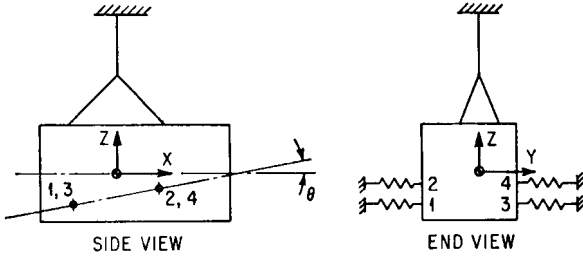


FIGURE 3.9 Method of determining the product of inertia with respect to the axes X and Z when Y is a principal axis of inertia. The test body is oscillated about the vertical Z axis with torsional stiffness provided by the four springs acting in the Y direction at the points shown. There should be no net force on the test body in the Y direction due to a rotation about the Z axis. The angle θ is varied until, at some value of $\theta = \theta_0$, oscillations about X and Z are uncoupled. The angle θ_0 and the moment of inertia about the Z axis give I_{xz} by Eq. (3.28).

When the moments and product of inertia with respect to a pair of axes X and Z in a principal plane of inertia XZ are known, the orientation of a principal axis P is given by

$$\theta_p = \frac{1}{2} \tan^{-1} \left(\frac{2I_{xz}}{I_{zz} - I_{xx}} \right) \tag{3.29}$$

where θ_p is the counterclockwise angle from the X axis to the P axis. The second principal axis in this plane is at $\theta_p + 90^\circ$.

Consider the determination of products of inertia when the directions of all principal axes of inertia are unknown. In one method, the moments of inertia about two independent sets of three mutually perpendicular axes are measured, and the direction cosines between these sets of axes are known from the positions of the axes. The values for the six moments of inertia and the nine direction cosines are then substituted into Eqs. (3.16) and (3.17). The result is six linear equations in the six unknown products of inertia, from which the values of the desired products of inertia may be found by simultaneous solution of the equations. This method leads to experimental errors of relatively large magnitude because each product of inertia is, in general, a function of all six moments of inertia, each of which contains an experimental error.

An alternative method is based upon the knowledge that one of the principal moments of inertia of a body is the largest and another is the smallest that can be obtained for any axis through the center-of-gravity. A trial-and-error procedure can be used to locate the orientation of the axis through the center-of-gravity having the maximum and/or minimum moment of inertia. After one or both are located, the moments and products of inertia for any set of axes are found by the techniques previously discussed.

The products of inertia of a body also may be determined by rotating the body at a constant angular velocity Ω about an axis passing through the center-of-gravity, as illustrated in Fig. 3.10. This method is similar to the balancing machine technique used to balance a body dynamically (see Chap. 39). If the bearings are a distance l apart and the dynamic reactions F_x and F_y are measured, the products of inertia are

$$I_{xz} = -\frac{F_x l}{\Omega^2} \quad I_{yz} = -\frac{F_y l}{\Omega^2} \quad (3.30)$$

Limitations to this method are (1) the size of the body that can be accommodated by the balancing machine and (2) the angular velocity that the body can withstand without damage from centrifugal forces. If the angle between the Z axis and a principal axis of inertia is small, high rotational speeds may be necessary to measure the reaction forces accurately.

PROPERTIES OF RESILIENT SUPPORTS

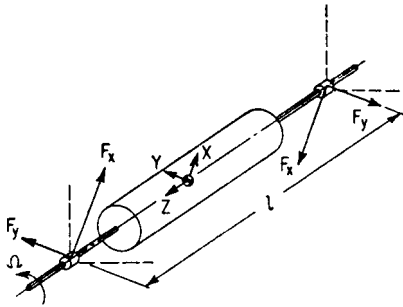


FIGURE 3.10 Balancing machine technique for determining products of inertia. The test body is rotated about the Z axis with angular velocity Ω . The dynamic reactions F_x and F_y , measured at the bearings, which are a distance l apart, give I_{xz} and I_{yz} by Eq. (3.30).

A resilient support is considered to be a three-dimensional element having two terminals or end connections. When the end connections are moved one relative to the other in any direction, the element resists such motion. In this chapter, the element is considered to be massless; the force that resists relative motion across the element is considered to consist of a spring force that is directly proportional to the relative displacement (deflection across the element) and a damping force that is directly proportional to the relative velocity (velocity across the element). Such an element is defined as a *linear resilient support*. Nonlinear elements are discussed in Chap. 4; elements with mass are discussed in Chap. 30; and nonlinear damping is discussed in Chaps. 2 and 30.

In a single degree-of-freedom system or in a system having constraints on the paths of motion of elements of the system (Chap. 2), the resilient element is constrained to deflect in a given direction and the properties of the element are defined with respect to the force opposing motion in this direction. In the absence of such constraints, the application of a force to a resilient element generally causes a motion in a different direction. The *principal elastic axes* of a resilient element are those axes for which the element, when unconstrained, experiences a deflection colinear with the direction of the applied force. Any axis of symmetry is a principal elastic axis.

In rigid body dynamics, the rigid body sometimes vibrates in modes that are coupled by the properties of the resilient elements as well as by their location. For example, if the body experiences a static displacement x in the direction of the X axis only, a resilient element opposes this motion by exerting a force $k_{xx}x$ on the body in the direction of the X axis, where one subscript on the spring constant k indicates the direction of the force exerted by the element and the other subscript indicates the direction of the deflection. If the X direction is not a principal elastic direction of the element and the body experiences a static displacement x in the X direction, the body is acted upon by a force $k_{yx}x$ in the Y direction if no displacement y is permitted. The stiffnesses have reciprocal properties; i.e., $k_{xy} = k_{yx}$. In general,

the stiffnesses in the directions of the coordinate axes can be expressed in terms of (1) principal stiffnesses and (2) the angles between the coordinate axes and the principal elastic axes of the element. (See Chap. 30 for a detailed discussion of a biaxial stiffness element.) Therefore, the stiffness of a resilient element can be represented pictorially by the combination of three mutually perpendicular, idealized springs oriented along the principal elastic directions of the resilient element. Each spring has a stiffness equal to the principal stiffness represented.

A resilient element is assumed to have damping properties such that each spring representing a value of principal stiffness is paralleled by an idealized viscous damper, each damper representing a value of principal damping. Hence, coupling through damping exists in a manner similar to coupling through stiffness. Consequently, the viscous damping coefficient c is analogous to the spring coefficient k ; i.e., the force exerted by the damping of the resilient element in response to a velocity \dot{x} is $c_{xx}\dot{x}$ in the direction of the X axis and $c_{yx}\dot{x}$ in the direction of the Y axis if \dot{y} is zero. Reciprocity exists; i.e., $c_{xy} = c_{yx}$.

The point of intersection of the principal elastic axes of a resilient element is designated as the *elastic center of the resilient element*. The elastic center is important since it defines the theoretical point location of the resilient element for use in the equations of motion of a resiliently supported rigid body. For example, the torque on the rigid body about the Y axis due to a force $k_{xx}x$ transmitted by a resilient element in the X direction is $k_{xx}a_zx$, where a_z is the Z coordinate of the elastic center of the resilient element.

In general, it is assumed that a resilient element is attached to the rigid body by means of "ball joints"; i.e., the resilient element is incapable of applying a couple to the body. If this assumption is not made, a resilient element would be represented not only by translational springs and dampers along the principal elastic axes but also by torsional springs and dampers resisting rotation about the principal elastic directions.

Figure 3.11 shows that the torsional elements usually can be neglected. The torque which acts on the rigid body due to a rotation β of the body and a rotation β of the support is $(k_t + a_z^2k_x)(\beta - \beta)$, where k_t is the torsional spring constant in the β direction. The torsional stiffness k_t usually is much smaller than $a_z^2k_x$ and can be neglected. Treatment of the general case indicates that if the torsional stiffnesses of the resilient element are small compared with the product of the translational stiffnesses times the square of distances from the elastic center of the resilient element to the center-of-gravity of the rigid body, the torsional stiffnesses have a negligible effect on the vibrational behavior of the body. The treatment of torsional dampers is completely analogous.

EQUATIONS OF MOTION FOR A RESILIENTLY SUPPORTED RIGID BODY

The differential equations of motion for the rigid body are given by Eqs. (3.2) and (3.3), where the \mathbf{F} 's and \mathbf{M} 's represent the forces and moments acting on the body, either directly or through the resilient supporting elements. Figure 3.12 shows a view of a rigid body at rest with an inertial set of axes $\bar{X}, \bar{Y}, \bar{Z}$ and a coincident set of axes X, Y, Z fixed in the rigid body, both sets of axes passing through the center-of-mass. A typical resilient element (2) is represented by parallel spring and viscous damper combinations arranged respectively parallel with the $\bar{X}, \bar{Y}, \bar{Z}$ axes. Another resilient element (1) is shown with its principal axes not parallel with $\bar{X}, \bar{Y}, \bar{Z}$.

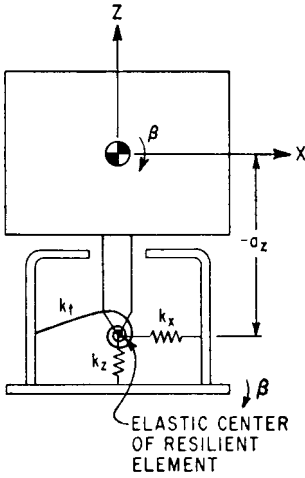


FIGURE 3.11 Pictorial representation of the properties of an undamped resilient element in the XZ plane including a torsional spring k_t . An analysis of the motion of the supported body in the XZ plane shows that the torsional spring can be neglected if $k_t \ll a_z^2 k_x$.

The displacement of the center-of-gravity of the body in the $\bar{X}, \bar{Y}, \bar{Z}$ directions is in Fig. 3.1 indicated by x_c, y_c, z_c , respectively; and rotation of the rigid body about these axes is indicated by α, β, γ , respectively. In Fig. 3.12, each resilient element is represented by three mutually perpendicular spring-damper combinations. One end of each such combination is attached to the rigid body; the other end is considered to be attached to a foundation whose corresponding translational displacement is defined by u, v, w in the $\bar{X}, \bar{Y}, \bar{Z}$ directions, respectively, and whose rotational displacement about these axes is defined by α, β, γ , respectively. The point of attachment of each of the idealized resilient elements is located at the coordinate distances a_x, a_y, a_z of the elastic center of the resilient element.

Consider the rigid body to experience a translational displacement x_c of its center-of-gravity and no other displacement, and neglect the effects of the

viscous dampers. The force developed by a resilient element has the effect of a force $-k_{xx}(x_c - u)$ in the X direction, a moment $k_{xx}(x_c - u)a_y$ in the γ coordinate (about the Z axis), and a moment $-k_{xx}(x_c - u)a_z$ in the β coordinate (about the Y axis). Furthermore, the coupling stiffness causes a force $-k_{xy}(x_c - u)$ in the Y direction and a force $-k_{xz}(x_c - u)$ in the Z direction. These forces have the moments $k_{xy}(x_c - u)a_z$ in the α coordinate; $-k_{xy}(x_c - u)a_x$ in the γ coordinate; $k_{xz}(x_c - u)a_x$ in the β coordinate; and $-k_{xz}(x_c - u)a_y$ in the α coordinate. By considering in a similar manner the forces and moments developed by a resilient element for successive displacements of the rigid body in the three translational and three rotational coordinates, and summing over the number of resilient elements, the equations of motion are written as follows:^{6,7}

$$\begin{aligned}
 m\ddot{x}_c + \Sigma k_{xx}(x_c - u) + \Sigma k_{xy}(y_c - v) + \Sigma k_{xz}(z_c - w) \\
 + \Sigma (k_{xz}a_y - k_{xy}a_z)(\alpha - \alpha) + \Sigma (k_{xx}a_z - k_{xz}a_x)(\beta - \beta) \\
 + \Sigma (k_{xy}a_x - k_{xx}a_y)(\gamma - \gamma) = F_x
 \end{aligned} \tag{3.31a}$$

$$\begin{aligned}
 I_{xx}\ddot{\alpha} - I_{xy}\ddot{\beta} - I_{xz}\ddot{\gamma} + \Sigma (k_{xz}a_y - k_{xy}a_z)(x_c - u) \\
 + \Sigma (k_{yz}a_y - k_{yy}a_z)(y_c - v) + \Sigma (k_{zz}a_y - k_{yz}a_z)(z_c - w) \\
 + \Sigma (k_{yy}a_z^2 + k_{zz}a_y^2 - 2k_{yz}a_ya_z)(\alpha - \alpha) \\
 + \Sigma (k_{xz}a_ya_z + k_{yz}a_xa_z - k_{zz}a_xa_y - k_{xy}a_z^2)(\beta - \beta) \\
 + \Sigma (k_{xy}a_ya_z + k_{yz}a_xa_y - k_{yy}a_xa_z - k_{xz}a_y^2)(\gamma - \gamma) = M_x
 \end{aligned} \tag{3.31b}$$

$$\begin{aligned}
 m\ddot{y}_c + \Sigma k_{xy}(x_c - u) + \Sigma k_{yy}(y_c - v) + \Sigma k_{yz}(z_c - w) \\
 + \Sigma (k_{yz}a_y - k_{yy}a_z)(\alpha - \alpha) + \Sigma (k_{xy}a_z - k_{yz}a_x)(\beta - \beta) \\
 + \Sigma (k_{yy}a_x - k_{xy}a_y)(\gamma - \gamma) = F_y
 \end{aligned} \tag{3.31c}$$

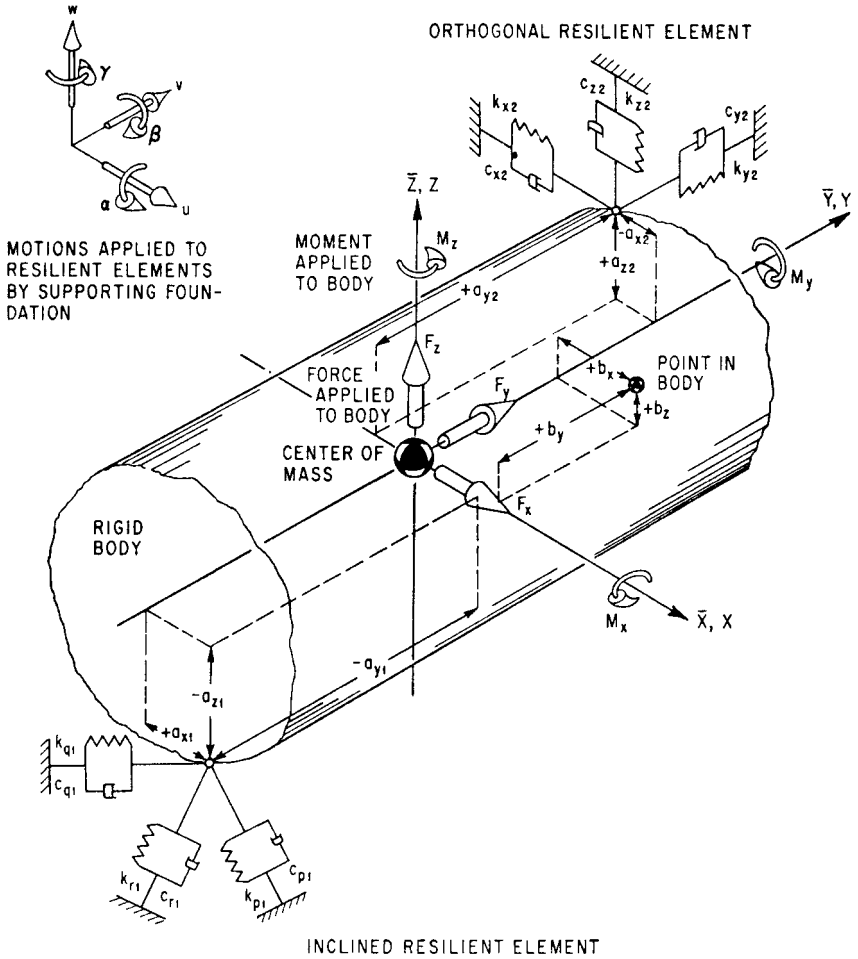


FIGURE 3.12 Rigid body at rest supported by resilient elements, with inertial axes $\bar{X}, \bar{Y}, \bar{Z}$ and coincident reference axes X, Y, Z passing through the center-of-mass. The forces F_x, F_y, F_z and the moments M_x, M_y, M_z are applied directly to the body; the translations u, v, w and rotations α, β, γ in and about the X, Y, Z axes, respectively, are applied to the resilient elements located at the coordinates a_x, a_y, a_z . The principal directions of resilient element (2) are parallel to the $\bar{X}, \bar{Y}, \bar{Z}$ axes (orthogonal), and those of resilient element (1) are not parallel to the $\bar{X}, \bar{Y}, \bar{Z}$ axes (inclined).

$$\begin{aligned}
 I_{yy}\ddot{\beta} - I_{xy}\ddot{\alpha} - I_{yz}\ddot{\gamma} + \Sigma(k_{xx}a_z - k_{xz}a_x)(x_c - u) \\
 + \Sigma(k_{xy}a_z - k_{yz}a_x)(y_c - v) + \Sigma(k_{xz}a_z - k_{zz}a_x)(z_c - w) \\
 + \Sigma(k_{xz}a_ya_z + k_{yz}a_xa_z - k_{zz}a_xa_y - k_{xy}a_z^2)(\alpha - \alpha) \\
 + \Sigma(k_{xx}a_z^2 + k_{zz}a_x^2 - 2k_{xz}a_xa_z)(\beta - \beta) \\
 + \Sigma(k_{xy}a_xa_z + k_{xz}a_xa_y - k_{xx}a_ya_z - k_{yz}a_x^2)(\gamma - \gamma) = M_y
 \end{aligned} \tag{3.31d}$$

$$\begin{aligned}
m\ddot{z}_c + \Sigma k_{xz}(x_c - u) + \Sigma k_{yz}(y_c - v) + \Sigma k_{zz}(z_c - w) \\
+ \Sigma(k_{zz}a_y - k_{yz}a_z)(\alpha - \alpha) + \Sigma(k_{xz}a_z - k_{zz}a_x)(\beta - \beta) \\
+ \Sigma(k_{yz}a_x - k_{xz}a_y)(\gamma - \gamma) = F_z
\end{aligned} \tag{3.31e}$$

$$\begin{aligned}
I_{zz}\ddot{\gamma} - I_{xz}\ddot{\alpha} - I_{yz}\ddot{\beta} + \Sigma(k_{xy}a_x - k_{xx}a_y)(x_c - u) \\
+ \Sigma(k_{yy}a_x - k_{xy}a_y)(y_c - v) + \Sigma(k_{yz}a_x - k_{xz}a_y)(z_c - w) \\
+ \Sigma(k_{xy}a_y a_z + k_{yz}a_x a_y - k_{yy}a_x a_z - k_{xz}a_y^2)(\alpha - \alpha) \\
+ \Sigma(k_{xy}a_x a_z + k_{xz}a_x a_y - k_{xx}a_y a_z - k_{yz}a_x^2)(\beta - \beta) \\
+ \Sigma(k_{xx}a_y^2 + k_{yy}a_x^2 - 2k_{xy}a_x a_y)(\gamma - \gamma) = M_z
\end{aligned} \tag{3.31f}$$

where the moments and products of inertia are defined by Eqs. (3.11) and (3.12) and the stiffness coefficients are defined as follows:

$$\begin{aligned}
k_{xx} &= k_p \lambda_{xp}^2 + k_q \lambda_{xq}^2 + k_r \lambda_{xr}^2 \\
k_{yy} &= k_p \lambda_{yp}^2 + k_q \lambda_{yq}^2 + k_r \lambda_{yr}^2 \\
k_{zz} &= k_p \lambda_{zp}^2 + k_q \lambda_{zq}^2 + k_r \lambda_{zr}^2 \\
k_{xy} &= k_p \lambda_{xp} \lambda_{yp} + k_q \lambda_{xq} \lambda_{yq} + k_r \lambda_{xr} \lambda_{yr} \\
k_{xz} &= k_p \lambda_{xp} \lambda_{zp} + k_q \lambda_{xq} \lambda_{zq} + k_r \lambda_{xr} \lambda_{zr} \\
k_{yz} &= k_p \lambda_{yp} \lambda_{zp} + k_q \lambda_{yq} \lambda_{zq} + k_r \lambda_{yr} \lambda_{zr}
\end{aligned} \tag{3.32}$$

where the λ 's are the cosines of the angles between the principal elastic axes of the resilient supporting elements and the coordinate axes. For example, λ_{xp} is the cosine of the angle between the X axis and the P axis of principal stiffness.

The equations of motion, Eqs. (3.31), do not include forces applied to the rigid body by damping forces from the resilient elements. To include damping, appropriate damping terms analogous to the corresponding stiffness terms are added to each equation. For example, Eq. (3.31a) would become

$$\begin{aligned}
m\ddot{x}_c + \Sigma c_{xx}(\dot{x}_c - \dot{u}) + \Sigma k_{xx}(x_c - u) + \dots \\
+ \Sigma(c_{xz}a_y - c_{xy}a_z)(\dot{\alpha} - \dot{\alpha}) + \Sigma(k_{xz}a_y - k_{xy}a_z)(\alpha - \alpha) + \dots = F_x \tag{3.31a'}
\end{aligned}$$

where

$$\begin{aligned}
c_{xx} &= c_p \lambda_{xp}^2 + c_q \lambda_{xq}^2 + c_r \lambda_{xr}^2 \\
c_{xy} &= c_p \lambda_{xp} \lambda_{yp} + c_q \lambda_{xq} \lambda_{yq} + c_r \lambda_{xr} \lambda_{yr}
\end{aligned}$$

The number of degrees-of-freedom of a vibrational system is the minimum number of coordinates necessary to define completely the positions of the mass elements of the system in space. The system of Fig. 3.12 requires a minimum of six coordinates $(x_c, y_c, z_c, \alpha, \beta, \gamma)$ to define the position of the rigid body in space; thus, the system is said to vibrate in six degrees-of-freedom. Equations (3.31) may be solved simultaneously for the three components x_c, y_c, z_c of the center-of-gravity displacement and the three components α, β, γ of the rotational displacement of the rigid body. In most practical instances, the equations are simplified considerably by one or more of the following simplifying conditions:

1. The reference axes X, Y, Z are selected to coincide with the principal inertial axes of the body; then

$$I_{xy} = I_{xz} = I_{yz} = 0 \quad (3.33)$$

2. The resilient supporting elements are so arranged that one or more planes of symmetry exist; i.e., motion parallel to the plane of symmetry has no tendency to excite motion perpendicular to it, or rotation about an axis lying in the plane does not excite motion parallel to the plane. For example, in Eq. (3.31a), motion in the XY plane does not tend to excite motion in the XZ or YZ plane if Σk_{xz} , $\Sigma(k_{xz}a_y - k_{xy}a_z)$, and $\Sigma(k_{xx}a_z - k_{xz}a_x)$ are zero.
3. The principal elastic axes P, Q, R of all resilient supporting elements are orthogonal with the reference axes X, Y, Z of the body, respectively. Then, in Eqs. (3.32),

$$\begin{aligned} k_{xx} &= k_p = k_x & k_{yy} &= k_q = k_y & k_{zz} &= k_r = k_z \\ k_{xy} &= k_{xz} = k_{yz} & & & & \end{aligned} \quad (3.34)$$

where k_x, k_y, k_z are defined for use when orthogonality exists. The supports are then called *orthogonal supports*.

4. The forces F_x, F_y, F_z and moments M_x, M_y, M_z are applied directly to the body and there are no motions ($u = v = w = \alpha = \beta = \gamma = 0$) of the foundation; or alternatively, the forces and moments are zero and excitation results from motion of the foundation.

In general, the effect of these simplifications is to reduce the numbers of terms in the equations and, in some instances, to reduce the number of equations that must be solved simultaneously. Simultaneous equations indicate coupled modes; i.e., motion cannot exist in one coupled mode independently of motion in other modes which are coupled to it.

MODAL COUPLING AND NATURAL FREQUENCIES

Several conditions of symmetry resulting from zero values for the product of inertia terms in Eq. (3.33) are discussed in the following sections.

ONE PLANE OF SYMMETRY WITH ORTHOGONAL RESILIENT SUPPORTS

When the YZ plane of the rigid body system in Fig. 3.12 is a plane of symmetry, the following terms in the equations of motion are zero:

$$\Sigma k_{yy} a_x = \Sigma k_{zz} a_x = \Sigma k_{yy} a_x a_z = \Sigma k_{zz} a_x a_y = 0 \quad (3.35)$$

Introducing the further simplification that the principal elastic axes of the resilient elements are parallel with the reference axes, Eqs. (3.34) apply. Then the motions in the three coordinates y_c, z_c, α are coupled but are independent of motion in any of the other coordinates; furthermore, the other three coordinates x_c, β, γ also are coupled. For example, Fig. 3.13 illustrates a resiliently supported rigid body, wherein the YZ plane is a plane of symmetry that meets the requirements of Eq. (3.35). The three natural frequencies for the y_c, z_c, α coupled directions are found by solving Eqs.

(3.31b), (3.31c), and (3.31e) [or Eqs. (3.31a), (3.31d), and (3.31f) for the x_c, β, γ coupled directions] simultaneously.⁶

$$\left(\frac{f_n}{f_z}\right)^6 - A\left(\frac{f_n}{f_z}\right)^4 + B\left(\frac{f_n}{f_z}\right)^2 - C = 0 \quad (3.36)$$

where

$$f_z = \frac{1}{2\pi} \sqrt{\frac{\Sigma k_z}{m}} \quad (3.37)$$

is a quantity having mathematical rather than physical significance if translational motion in the direction of the Z axis is coupled to other modes of motion. (Such coupling exists for the system of Fig. 3.13.) The roots f_n represent the natural frequencies of the system in the coupled modes. The coefficients A, B, C for the coupled modes in the y_c, z_c, α coordinates are

$$A_{y\alpha} = 1 + \frac{\Sigma k_y}{\Sigma k_z} + D_{zx}$$

$$B_{y\alpha} = D_{zx} + \frac{\Sigma k_y}{\Sigma k_z} (1 + D_{zx}) - \frac{(\Sigma k_y a_z)^2 + (\Sigma k_z a_y)^2}{\rho_x^2 (\Sigma k_z)^2}$$

$$C_{y\alpha} = \frac{\Sigma k_y}{\Sigma k_z} \left(D_{zx} - \frac{(\Sigma k_z a_y)^2}{\rho_x^2 (\Sigma k_z)^2} \right) - \frac{(\Sigma k_y a_z)^2}{\rho_x^2 (\Sigma k_z)^2}$$

where

$$D_{zx} = \frac{\Sigma k_y a_z^2 + \Sigma k_z a_y^2}{\rho_x^2 \Sigma k_z}$$

and ρ_x is the radius of gyration of the rigid body with respect to the X axis.

The corresponding coefficients for the coupled modes in the x_c, β, γ coordinates are

$$A_{x\beta\gamma} = \frac{\Sigma k_x}{\Sigma k_z} + D_{zy} + D_{zz}$$

$$B_{x\beta\gamma} = \frac{\Sigma k_x}{\Sigma k_z} (D_{zy} + D_{zz}) + D_{zy} D_{zz}$$

$$- \frac{(\Sigma k_x a_z)^2}{\rho_y^2 (\Sigma k_z)^2} - \frac{(\Sigma k_x a_y)^2}{\rho_z^2 (\Sigma k_z)^2} - \frac{(\Sigma k_x a_y a_z)^2}{\rho_y^2 \rho_z^2 (\Sigma k_z)^2}$$

$$C_{x\beta\gamma} = \frac{\Sigma k_x}{\Sigma k_z} \left[D_{zy} D_{zz} - \frac{(\Sigma k_x a_y a_z)^2}{\rho_y^2 \rho_z^2 (\Sigma k_z)^2} \right] - \frac{(\Sigma k_x a_y)^2}{\rho_z^2 (\Sigma k_z)^2} D_{zy}$$

$$- \frac{(\Sigma k_x a_z)^2}{\rho_y^2 (\Sigma k_z)^2} D_{zz} + 2 \frac{(\Sigma k_x a_y)(\Sigma k_x a_z)(\Sigma k_y a_x)}{\rho_y^2 \rho_z^2 (\Sigma k_z)^3}$$

where

$$D_{zy} = \frac{\Sigma k_x a_z^2 + \Sigma k_z a_x^2}{\rho_y^2 \Sigma k_z} \quad D_{zz} = \frac{\Sigma k_x a_y^2 + \Sigma k_y a_x^2}{\rho_z^2 \Sigma k_z}$$

and ρ_y, ρ_z are the radii of gyration of the rigid body with respect to the Y, Z axes.

The roots of the cubic equation Eq. (3.36) may be found graphically from Fig. 3.14.⁶ The coefficients A, B, C are first calculated from the above relations for the appropriate set of coupled coordinates. Figure 3.14 is entered on the abscissa scale at the appropriate value for the quotient B/A^2 . Small values of B/A^2 are in Fig. 3.14A, and large values in Fig. 3.14B. The quotient C/A^3 is the parameter for the family of curves. Upon selecting the appropriate curve, three values of $(f_n/f_z)/\sqrt{A}$

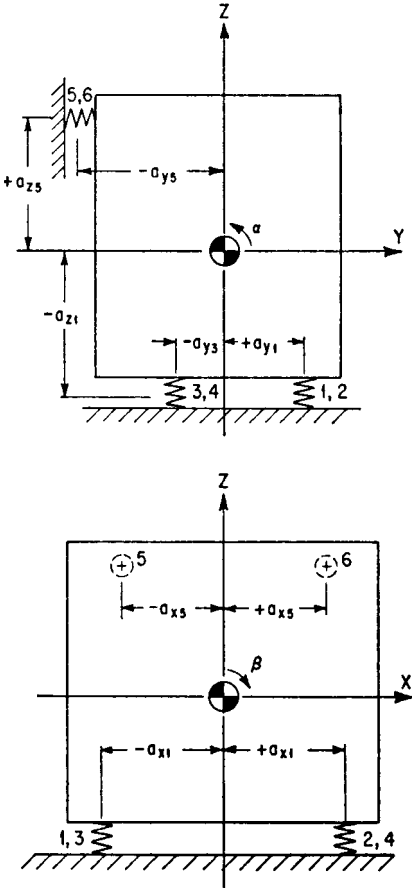


FIGURE 3.13 Example of a rigid body on orthogonal resilient supporting elements with one plane of symmetry. The YZ plane is a plane of symmetry since each resilient element has properties identical to those of its mirror image in the YZ plane; i.e., $k_{x1} = k_{x2}$, $k_{x3} = k_{x4}$, $k_{x5} = k_{x6}$, etc. The conditions satisfied are Eqs. (3.33) to (3.35).

(3.31b) and (3.31c)]. The planes of symmetry are the XZ and YZ planes. For example, a common system is illustrated in Fig. 3.15, where four identical resilient supporting elements are located symmetrically about the Z axis in a plane not containing the center-of-gravity.⁶ Coupling exists between translation in the X direction and rotation about the Y axis (x_c, β), as well as between translation in the Y direction and rotation about the X axis (y_c, α). Translation in the Z direction (z_c) and rotation about the Z axis (γ) are each independent of all other modes.

The natural frequency in the Z direction is found by solving Eq. (3.31e) to obtain Eq. (3.37), where $\Sigma k_{zz} = 4k_z$. The rotational natural frequency f_γ about the Z axis is found by solving Eq. (3.31f); it can be expressed with respect to the natural frequency in the direction of the Z axis:

are read from the ordinate and transferred to the left scale of the nomograph in Fig. 3.14B. Diagonal lines are drawn for each root to the value of A on the right scale, as indicated by dotted lines, and the roots f_n/f_z of the equation are indicated by the intercept of these dotted lines with the center scale of the nomograph.

The coefficients A, B, C can be simplified if all resilient elements have equal stiffness in the same direction. The stiffness coefficients always appear to equal powers in numerator and denominator, and lead to dimensionless ratios of stiffness. For n resilient elements, typical terms reduce as follows:

$$\frac{\Sigma k_y}{\Sigma k_z} = \frac{k_y}{k_z} \quad \frac{\Sigma k_z a_y^2}{\rho_x^2 \Sigma k_z} = \frac{\Sigma a_y^2}{n \rho_x^2}$$

$$\frac{(\Sigma k_x a_y a_z)^2}{\rho_y^2 \rho_z^2 (\Sigma k_z)^2} = \left(\frac{k_x}{n k_z} \frac{\Sigma a_y a_z}{\rho_y \rho_z} \right)^2, \text{ etc.}$$

TWO PLANES OF SYMMETRY WITH ORTHOGONAL RESILIENT SUPPORTS

Two planes of symmetry may be achieved if, in addition to the conditions of Eqs. (3.33) to (3.35), the following terms of Eqs. (3.31) are zero:

$$\Sigma k_{xx} a_y = \Sigma k_{zz} a_y = \Sigma k_{xx} a_y a_z = 0 \tag{3.38}$$

Under these conditions, Eqs. (3.31) separate into two independent equations, Eqs. (3.31e) and (3.31f), and two sets each consisting of two coupled equations [Eqs. (3.31a) and (3.31d); Eqs.

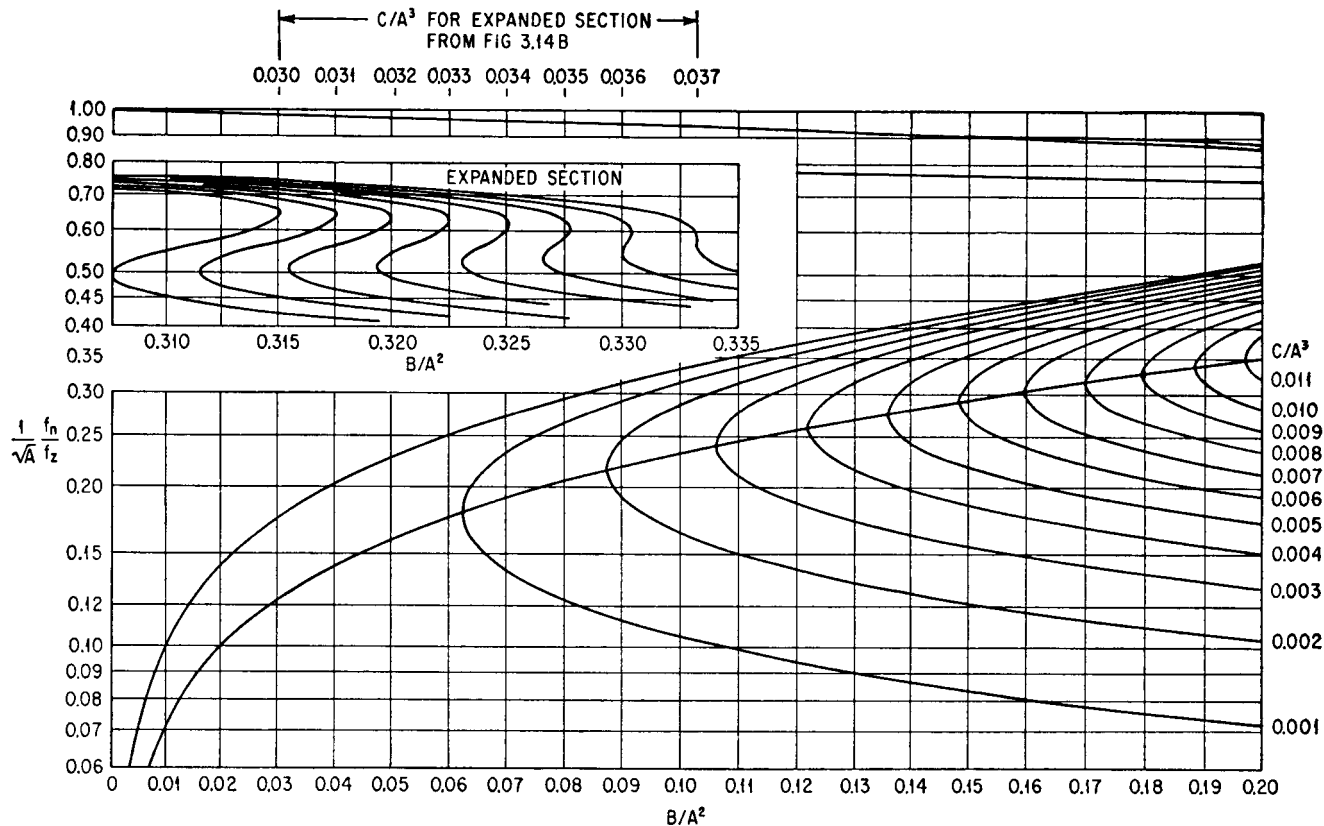


FIGURE 3.14A Graphical method of determining solutions of the cubic Eq. (3.36). Calculate A , B , C for the appropriate set of coupled coordinates, enter the abscissa at B/A^2 (values less than 0.2 on Fig. 3.14A, values greater than 0.2 on Fig. 3.14B), and read three values of $(f_n/f_z)/\sqrt{A}$ from the curve having the appropriate value of C/A^3 .

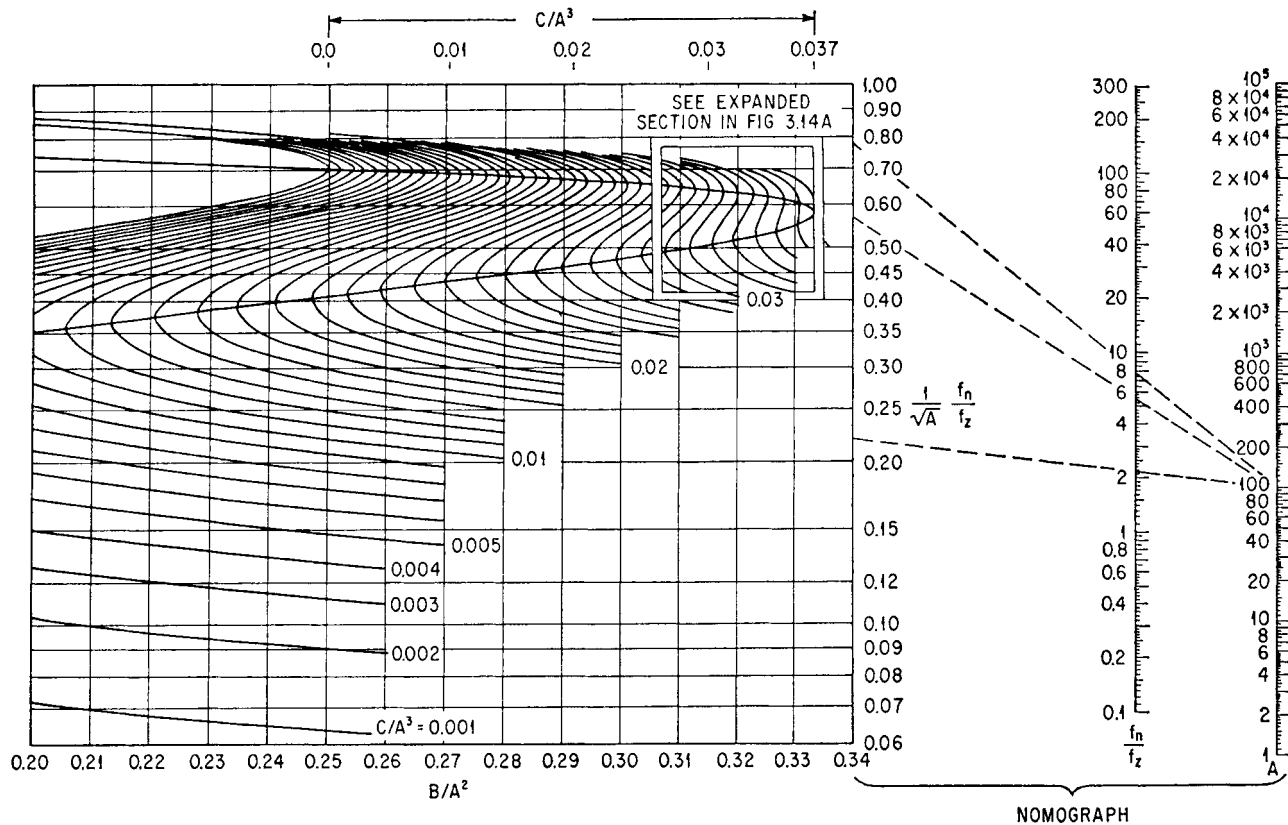


FIGURE 3.14B Using the above nomograph with values of $(f_n/f_z)/\sqrt{A}$ (see Fig. 3.14A), a diagonal line is drawn from each value of $(f_n/f_z)/\sqrt{A}$ on the left scale of the nomograph to the value of A on the right scale, as indicated by the dotted lines. The three roots f_n/f_z of Eq. (3.36) are given by the intercept of these dotted lines with the center scale of the nomograph. (After F. F. Vane.⁶)

$$\frac{f_y}{f_z} = \sqrt{\frac{k_x}{k_z} \left(\frac{a_y}{\rho_z}\right)^2 + \frac{k_y}{k_z} \left(\frac{a_x}{\rho_z}\right)^2} \tag{3.39}$$

where ρ_z is the radius of gyration with respect to the Z axis.

The natural frequencies in the coupled x_c, β modes are found by solving Eqs. (3.31a) and (3.31d) simultaneously; the roots yield the following expression for natural frequency:

$$\frac{f_{x\beta}^2}{f_z^2} = \frac{1}{2} \left\{ \frac{k_x}{k_z} \left(1 + \frac{a_z^2}{\rho_y^2}\right) + \frac{a_x^2}{\rho_y^2} \pm \sqrt{\left[\frac{k_x}{k_z} \left(1 + \frac{a_z^2}{\rho_y^2}\right) + \frac{a_x^2}{\rho_y^2}\right]^2 - 4 \frac{k_x}{k_z} \frac{a_x^2}{\rho_y^2}} \right\} \tag{3.40}$$

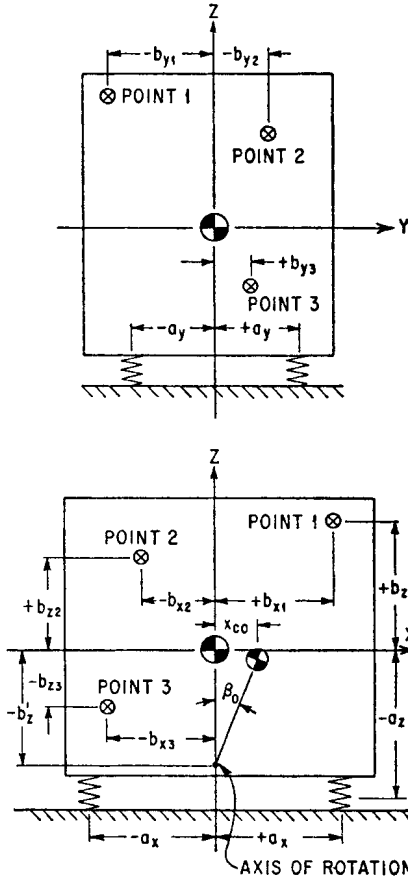


FIGURE 3.15 Example of a rigid body on orthogonal resilient supporting elements with two planes of symmetry. The XZ and YZ planes are planes of symmetry since the four resilient supporting elements are identical and are located symmetrically about the Z axis. The conditions satisfied are Eqs. (3.33), (3.34), (3.35), and (3.38). At any single frequency, coupled vibration in the x_c, β direction due to X vibration of the foundation is equivalent to a pure rotation of the rigid body with respect to an axis of rotation as shown. Points 1, 2, and 3 refer to the example of Fig. 3.26.

Figure 3.16 provides a convenient graphical method for determining the two coupled natural frequencies $f_{x\beta}$. An expression similar to Eq. (3.40) is obtained for $f_{y\alpha}^2/f_z^2$ by solving Eqs. (3.31b) and (3.31d) simultaneously. By replacing $\rho_y, a_x, k_x, f_{x\beta}$ with $\rho_x, a_y, k_y, f_{y\alpha}$, respectively, Fig. 3.16 also can be used to determine the two values of $f_{y\alpha}$.

It may be desirable to select resilient element locations a_x, a_y, a_z which will produce coupled natural frequencies in specified frequency ranges, with resilient elements having specified stiffness ratios $k_x/k_z, k_y/k_z$. For this purpose it is convenient to plot solutions of Eq. (3.40) in the form shown in Figs. 3.17 to 3.19. These plots are termed *space-plots* and their use is illustrated in Example 3.1.⁸

The space-plots are derived as follows: In general, the two roots of Eq. (3.40) are numerically different, one usually being greater than unity and the other less than unity. Designating the root associated with the positive sign before the radical (higher value) as f_h/f_z , Eq. (3.40) may be written in the following form:

$$\frac{(a_x/\rho_y)^2}{(f_h/f_z)^2} + \frac{(a_z/\rho_y)^2}{(k_z/k_x)(f_h/f_z)^2 - 1} = 1 \tag{3.40a}$$

Equation (3.40a) is shown graphically by the large ellipses about the center of Figs. 3.17 to 3.19, for stiffness ratios k_x/k_z

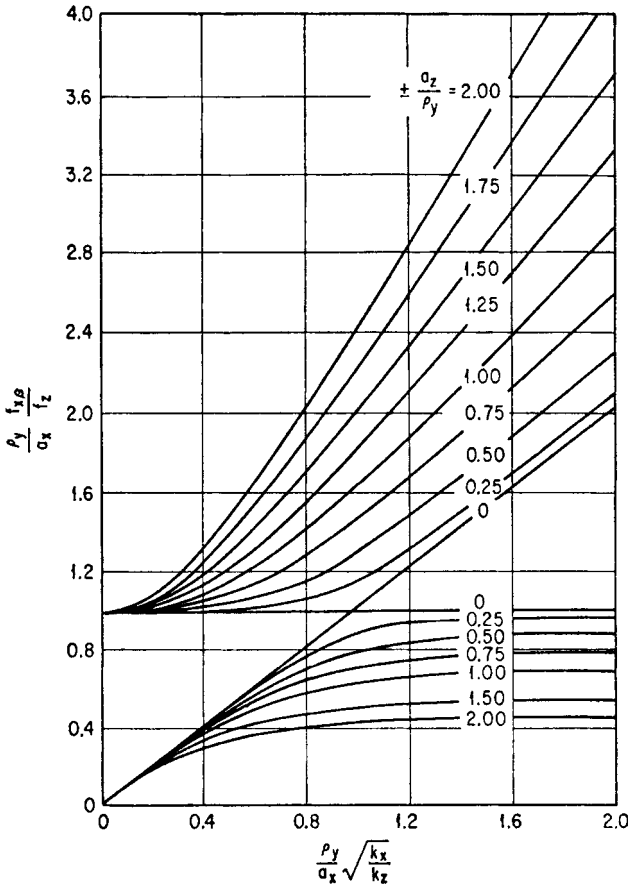


FIGURE 3.16 Curves showing the ratio of each of the two coupled natural frequencies $f_{x\beta}$ to the decoupled natural frequency f_z , for motion in the XZ plane of symmetry for the system in Fig. 3.15 [see Eq. (3.40)]. Calculate the abscissa $(\rho_y/a_x) \sqrt{k_x/k_z}$ and the parameter a_z/ρ_y , where a_x , a_z are indicated in Fig. 3.15; k_x , k_z are the stiffnesses of the resilient supporting elements in the X , Z directions, respectively; and ρ_y is the radius of gyration of the body about the Y axis. The two values read from the ordinate when divided by ρ_y/a_x give the natural frequency ratios $f_{x\beta}/f_z$.

of $1/2$, 1, and 2, respectively. A particular type of resilient element tends to have a constant stiffness ratio k_x/k_z ; thus, Figs. 3.17 to 3.19 may be used by cut-and-try methods to find the coordinates a_x , a_z of such elements to attain a desired value of f_h .

Designating the root of Eq. (3.40) associated with the negative sign (lower value) by f_b , Eq. (3.40) may be written as follows:

$$\frac{(a_x/\rho_y)^2}{(f_b/f_x)^2} - \frac{(a_z/\rho_y)^2}{1 - (k_z/k_x)(f_b/f_z)^2} = 1 \tag{3.40b}$$

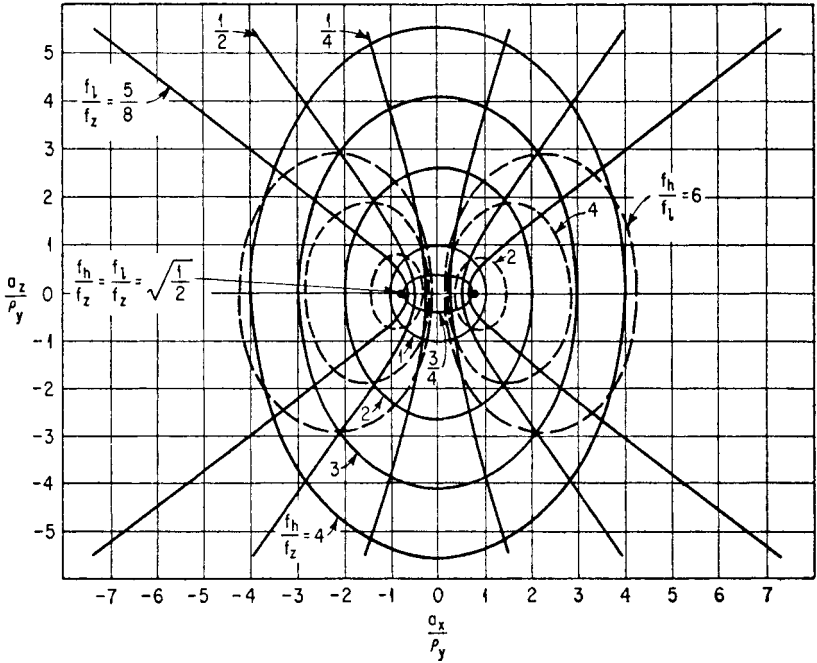


FIGURE 3.17 Space-plot for the system in Fig. 3.15 when the stiffness ratio $k_x/k_z = 0.5$, obtained from Eqs. (3.40a) to (3.40c). With all dimensions divided by the radius of gyration ρ_y about the Y axis, superimpose the outline of the rigid body in the XZ plane on the plot; the center-of-gravity of the body is located at the coordinate center of the plot. The elastic centers of the resilient supporting elements give the natural frequency ratios f_l/f_z , f_l/f_x , and f_h/f_l for x_o, β coupled motion, each ratio being read from one of the three families of curves as indicated on the plot. Replacing k_x, ρ_y, a_x with k_y, ρ_z, a_y , respectively, allows the plot to be applied to motions in the YZ plane.

Equation (3.40b) is shown graphically by the family of hyperbolas on each side of the center in Figs. 3.17 to 3.19, for values of the stiffness ratio k_x/k_z of $1/2, 1$, and 2 .

The two roots f_h/f_z and f_l/f_z of Eq. (3.40) may be expressed as the ratio of one to the other. This relationship is given parametrically as follows:

$$\left[\frac{2 \frac{a_x}{\rho_y} \pm \sqrt{\frac{k_x}{k_z} \left(\frac{f_h}{f_l} + \frac{f_l}{f_h} \right)}}{\sqrt{\frac{k_x}{k_z} \left(\frac{f_h}{f_l} - \frac{f_l}{f_h} \right)}} \right]^2 + \left[\frac{2 \frac{a_z}{\rho_y}}{\frac{f_h}{f_l} - \frac{f_l}{f_h}} \right]^2 = 1 \tag{3.40c}$$

Equation (3.40c) is shown graphically by the smaller ellipses (shown dotted) displaced from the vertical center line in Figs. 3.17 to 3.19.

Example 3.1. A rigid body is symmetrical with respect to the XZ plane; its width in the X direction is 13 in. and its height in the Z direction is 12 in. The center-of-gravity is $5\frac{1}{2}$ in. from the lower side and $6\frac{3}{4}$ in. from the right side. The radius of gyration about the Y axis through the center-of-gravity is 5.10 in. Use a space-plot to evaluate the effects of the location for attachment of resilient supporting elements having the characteristic stiffness ratio $k_x/k_z = 1/2$.

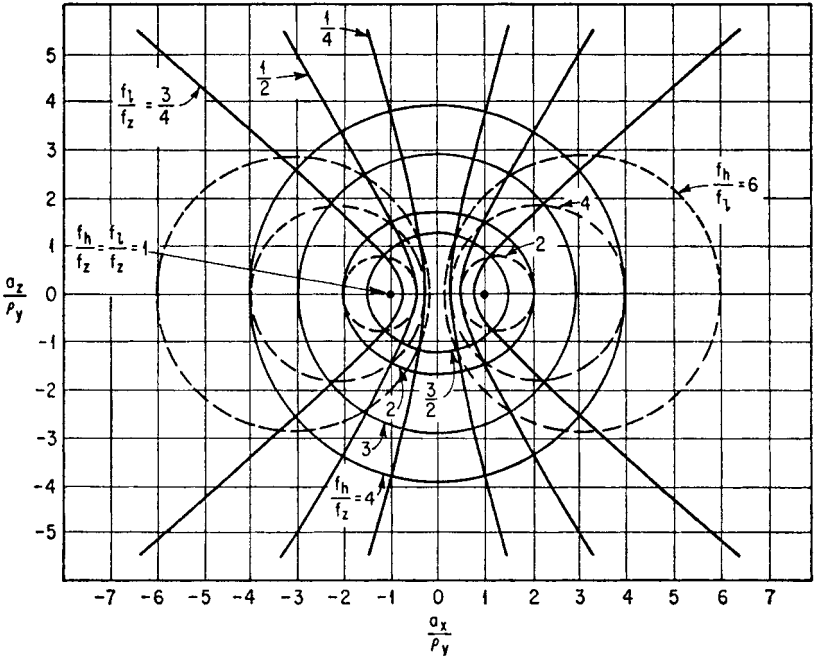


FIGURE 3.18 Space-plot for the system in Fig. 3.15 when the stiffness ratio $k_x/k_z = 1$. See caption for Fig. 3.17.

Superimpose the outline of the body on the space-plot of Fig. 3.20, with its center-of-gravity at the coordinate center of the plot. (Figure 3.20 is an enlargement of the central portion of Fig. 3.17.) All dimensions are divided by the radius of gyration ρ_y . Thus, the four corners of the body are located at coordinate distances as follows:

Upper right corner:

$$\frac{a_z}{\rho_y} = \frac{+6.50}{5.10} = +1.28 \qquad \frac{a_x}{\rho_y} = \frac{+6.75}{5.10} = +1.32$$

Upper left corner:

$$\frac{a_z}{\rho_y} = \frac{+6.50}{5.10} = +1.28 \qquad \frac{a_x}{\rho_y} = \frac{-6.25}{5.10} = -1.23$$

Lower right corner:

$$\frac{a_z}{\rho_y} = \frac{-5.50}{5.10} = -1.08 \qquad \frac{a_x}{\rho_y} = \frac{+6.75}{5.10} = +1.32$$

Lower left corner:

$$\frac{a_z}{\rho_y} = \frac{-5.50}{5.10} = -1.08 \qquad \frac{a_x}{\rho_y} = \frac{-6.25}{5.10} = -1.23$$

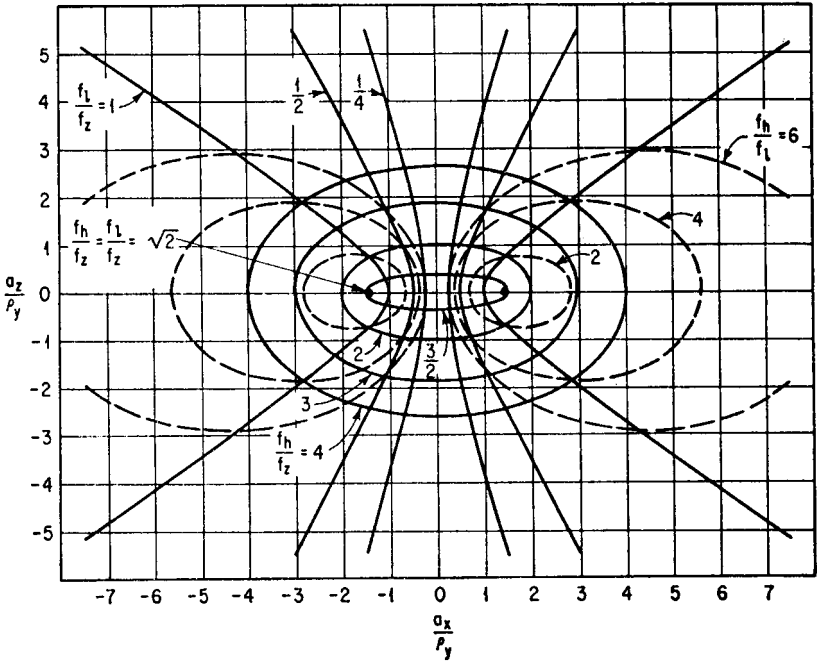


FIGURE 3.19 Space-plot for the system in Fig. 3.15 when the stiffness ratio $k_x/k_z = 2$. See caption for Fig. 3.17.

The resilient supports are shown in heavy outline at A in Fig. 3.20, with their elastic centers indicated by the solid dots. The horizontal coordinates of the resilient supports are $a_x/\rho_y = \pm 0.59$, or $a_x = \pm 0.59 \times 5.10 = \pm 3$ in. from the vertical coordinate axis. The corresponding natural frequencies are $f_h/f_z = 1.25$ (from the ellipses) and $f_i/f_z = 0.33$ (from the hyperbolas). An alternative position is indicated by the hollow circles B . The natural frequencies for this position are $f_h/f_z = 1.43$ and $f_i/f_z = 0.50$. The natural frequency f_z in vertical translation is found from the mass of the equipment and the summation of stiffnesses in the Z direction, using Eq. (3.37). This example shows how space-plots make it possible to determine the locations of the resilient elements required to achieve given values of the coupled natural frequencies with respect to f_z .

THREE PLANES OF SYMMETRY WITH ORTHOGONAL RESILIENT SUPPORTS

A system with three planes of symmetry is defined by six independent equations of motion. A system having this property is sometimes called a *center-of-gravity system*. The equations are derived from Eqs. (3.31) by substituting, in addition to the conditions of Eqs. (3.33), (3.34), (3.35), and (3.38), the following condition:

$$\sum k_{xx} a_z = \sum k_{yy} a_z = 0 \tag{3.41}$$

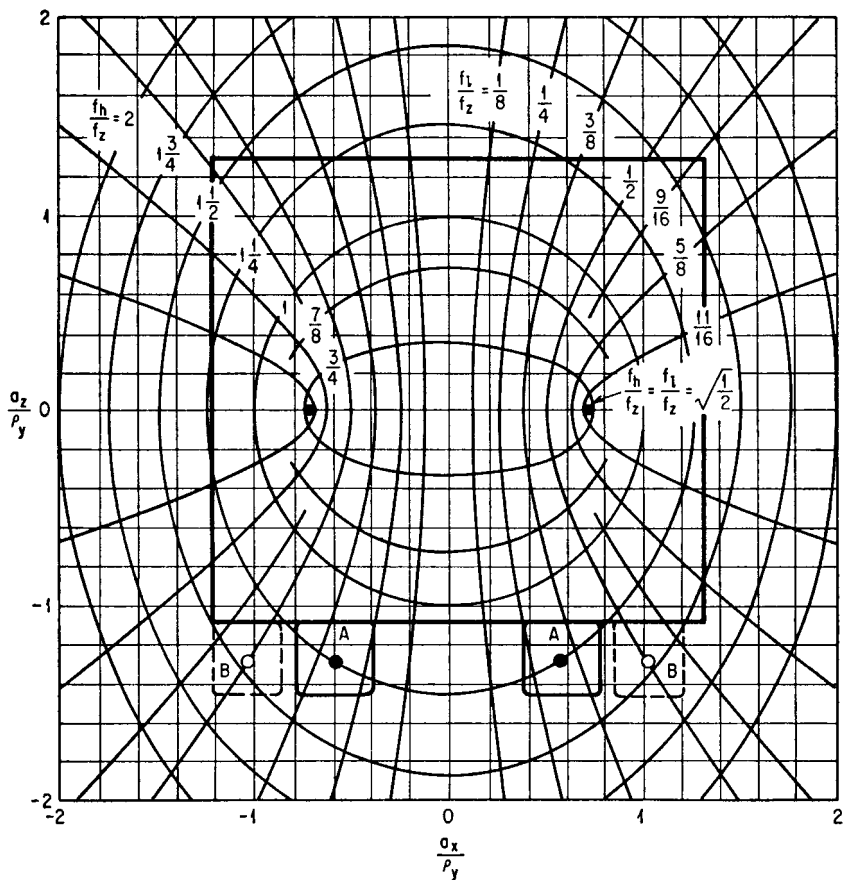


FIGURE 3.20 Enlargement of the central portion of Fig. 3.17 with the outline of the rigid body discussed in Example 3.1.

The resulting six independent equations define six uncoupled modes of vibration, three in translation and three in rotation. The natural frequencies are:

Translation along *X* axis:

$$f_x = \frac{1}{2\pi} \sqrt{\frac{\sum k_x}{m}}$$

Translation along *Y* axis:

$$f_y = \frac{1}{2\pi} \sqrt{\frac{\sum k_y}{m}}$$

Translation along *Z* axis:

$$f_z = \frac{1}{2\pi} \sqrt{\frac{\sum k_z}{m}}$$

Rotation about X axis:

$$f_\alpha = \frac{1}{2\pi} \sqrt{\frac{\Sigma(k_y a_z^2 + k_z a_y^2)}{m \rho_x^2}} \tag{3.42}$$

Rotation about Y axis:

$$f_\beta = \frac{1}{2\pi} \sqrt{\frac{\Sigma(k_x a_z^2 + k_z a_x^2)}{m \rho_y^2}}$$

Rotation about Z axis:

$$f_\gamma = \frac{1}{2\pi} \sqrt{\frac{\Sigma(k_x a_y^2 + k_y a_x^2)}{m \rho_z^2}}$$

TWO PLANES OF SYMMETRY WITH RESILIENT SUPPORTS INCLINED IN ONE PLANE ONLY

When the principal elastic axes of the resilient supporting elements are inclined with respect to the X, Y, Z axes, the stiffness coefficients k_{xy} , k_{xz} , k_{yz} are nonzero. This introduces elastic coupling, which must be considered in evaluating the equations of motion. Two planes of symmetry may be achieved by meeting the conditions of Eqs. (3.33), (3.35), and (3.38). For example, consider the rigid body supported by four identical resilient supporting elements located symmetrically about the Z axis, as shown in Fig. 3.21. The XZ and the YZ planes are planes of symmetry, and the resilient elements are inclined toward the YZ plane so that one of their principal elastic axes R is inclined at the angle ϕ with the Z direction as shown; hence $k_{yy} = k_q$, and $k_{xy} = k_{yz} = 0$.

Because of symmetry, translational motion z_c in the Z direction and rotation γ about the Z axis are each decoupled from the other modes. The pairs of translational and rotational modes in the x_c , β and y_c , α coordinates are coupled. The natural frequency in the Z direction is

$$f_z = \sqrt{\frac{k_p}{k_r} \sin^2 \phi + \cos^2 \phi} \tag{3.43}$$

where f_r is a fictitious natural frequency used for convenience only; it is related to Eq. (3.37) wherein $4k_r$ is substituted for Σk_c :

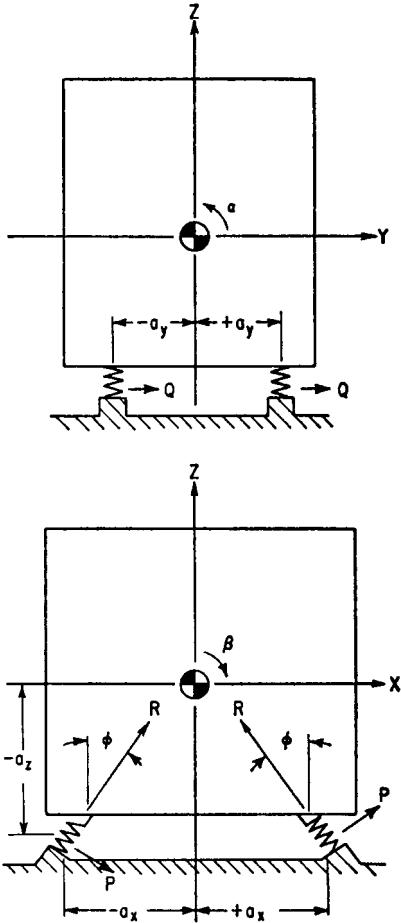


FIGURE 3.21 Example of a rigid body on resilient supporting elements inclined toward the YZ plane. The resilient supporting elements are identical and are located symmetrically about the Z axis, making XZ and YZ planes of symmetry. The principal stiffnesses in the XZ plane are k_p and k_r . The conditions satisfied are Eqs. (3.33), (3.35), and (3.38).

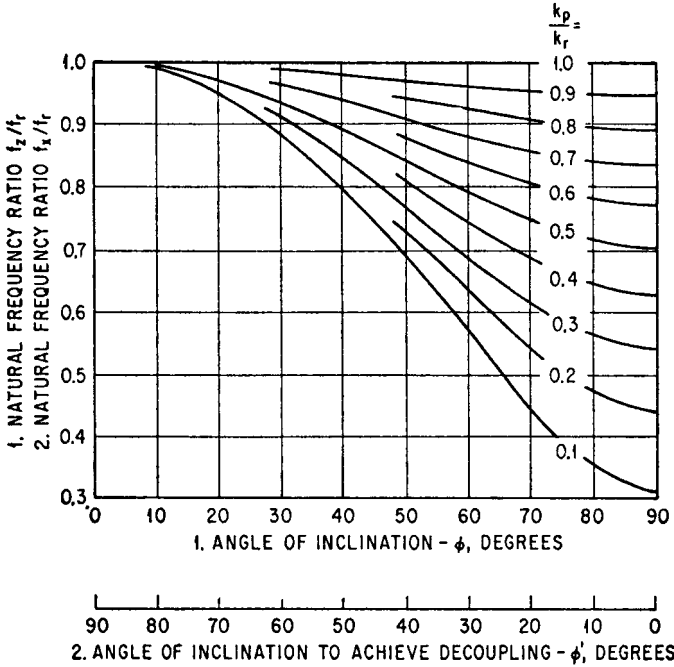


FIGURE 3.22 Curves showing the ratio of the decoupled natural frequency f_z of translation z_c to the fictitious natural frequency f_r for the system shown in Fig. 3.21 [see Eq. (3.43)] when the resilient supporting elements are inclined at the angle ϕ . The curves also indicate the ratio of the decoupled natural frequency f_x of translation x_c to f_r when ϕ has a value ϕ' (use lower abscissa scale) which decouples x_c, β motions [see Eqs. (3.47) and (3.48)].

$$f_r = \frac{1}{2\pi} \sqrt{\frac{4k_r}{m}}$$

Equation (3.43) is plotted in Fig. 3.22, where the angle ϕ is indicated by the upper of the abscissa scales.

The rotational natural frequency about the Z axis is obtained from

$$\frac{f_z}{f_r} = \sqrt{\left(\frac{k_p}{k_r} \cos^2 \phi + \sin^2 \phi\right) \left(\frac{a_y}{\rho_z}\right)^2 + \frac{k_q}{k_r} \left(\frac{a_x}{\rho_z}\right)^2} \tag{3.44}$$

For the x_c, β coupled mode, the two natural frequencies are

$$\frac{f_{x\beta}}{f_r} = \frac{1}{2} \left[A \pm \sqrt{A^2 - 4 \frac{k_p}{k_r} \left(\frac{a_x}{a_y}\right)^2} \right] \tag{3.45}$$

where
$$A = \left(\frac{k_p}{k_r} \cos^2 \phi + \sin^2 \phi\right) \left[1 + \left(\frac{a_z}{\rho_y}\right)^2 \right] + \left(\frac{k_p}{k_r} \sin^2 \phi + \cos^2 \phi\right) \left(\frac{a_x}{\rho_y}\right)^2 + 2 \left(1 - \frac{k_p}{k_r}\right) \left| \frac{a_x}{\rho_y} \right| \sin \phi \cos \phi$$

For the y_c, α coupled mode, the natural frequencies are

$$\frac{f_{y\alpha}}{f_r} = \frac{1}{2} \left[B \pm \sqrt{B^2 - 4 \frac{k_q}{k_r} \left(\frac{k_p}{k_r} \sin^2 \phi + \cos^2 \phi \right) \left(\frac{a_y}{\rho_x} \right)^2} \right] \quad (3.46)$$

where

$$B = \frac{k_q}{k_r} \left[1 + \left(\frac{a_z}{\rho_x} \right)^2 \right] + \left(\frac{k_p}{k_r} \sin^2 \phi + \cos^2 \phi \right) \left(\frac{a_y}{\rho_x} \right)^2$$

DECOUPLING OF MODES IN A PLANE USING INCLINED RESILIENT SUPPORTS

The angle ϕ of inclination of principal elastic axes (see Fig. 3.21) can be varied to produce changes in the amount of coupling between the x_c and β coordinates. Decoupling of the x_c and β coordinates is effected if

$$\left| \frac{a_z}{a_x} \right| = \frac{[1 - (k_p/k_r)] \cot \phi'}{1 + (k_p/k_r) \cot^2 \phi'} \quad (3.47)$$

where ϕ' is the value of the angle of inclination ϕ required to achieve decoupling. When Eq. (3.47) is satisfied, the configuration is sometimes called an "equivalent center-of-gravity system" in the YZ plane since all modes of motion in that plane are decoupled. Figure 3.23 is a graphical presentation of Eq. (3.47). There may be two values of ϕ' that decouple the x_c and β modes for any combination of stiffness and location for the resilient supporting elements.

The decoupled natural frequency for translation in the X direction is obtained from

$$\frac{f_x}{f_r} = \sqrt{\frac{k_p}{k_r} \cos^2 \phi' + \sin^2 \phi'} \quad (3.48)$$

The relation of Eq. (3.48) is shown graphically in Fig. 3.22 where the angle ϕ' is indicated by the lower of the abscissa scales. The natural frequency in the β mode is obtained from

$$\frac{f_\beta}{f_r} = \frac{a_x}{\rho_y} \sqrt{\frac{1}{(k_r/k_p) \sin^2 \phi' + \cos^2 \phi'}} \quad (3.49)$$

COMPLETE DECOUPLING OF MODES USING RADIALLY INCLINED RESILIENT SUPPORTS

In general, the analysis of rigid body motion with the resilient supporting elements inclined in more than one plane is quite involved. A particular case where sufficient symmetry exists to provide relatively simple yet useful results is the configuration illustrated in Fig. 3.24. From symmetry about the Z axis, $I_{xx} = I_{yy}$. Any number n of resilient supporting elements greater than 3 may be used. For clarity of illustration, the rigid body is shown as a right circular cylinder with $n = 3$.

The resilient supporting elements are arranged symmetrically about the Z axis; they are attached to one end face of the cylinder at a distance a_r from the Z axis and a distance a_z from the XY reference plane. The resilient elements are inclined so that their principal elastic axes R intersect at a common point on the Z axis; thus, the angle between the Z axis and the R axis for each element is ϕ . The principal elastic axes P

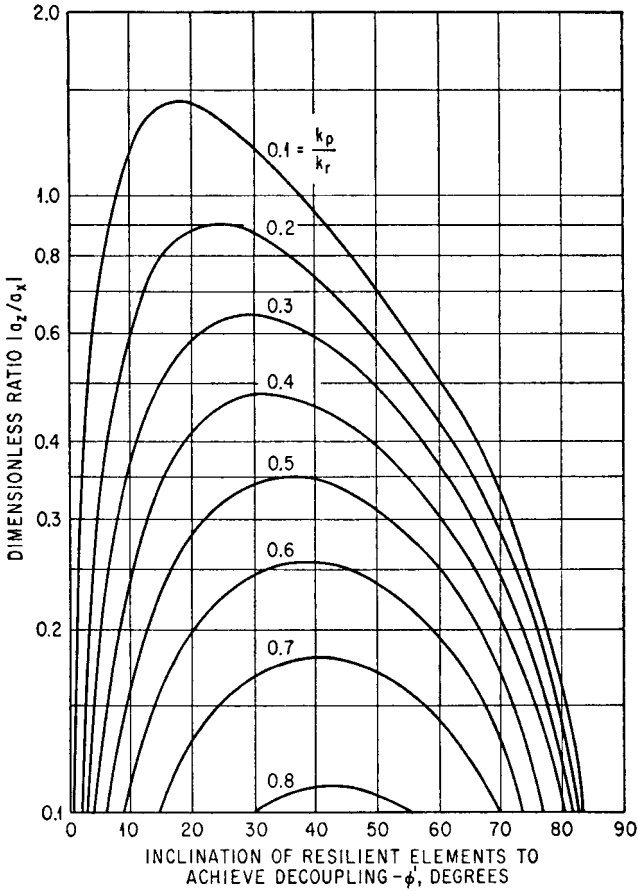


FIGURE 3.23 Curves showing the angle of inclination ϕ' of the resilient elements which achieves decoupling of the x_c, β motions in Fig. 3.21 [see Eq. (3.47)]. Calculate the ordinate $|a_z/a_x|$ and with the stiffness ratio k_p/k_r determine two values of ϕ' for which decoupling is possible. Decoupling is not possible for a particular value of k_p/k_r if $|a_z/a_x|$ has a value greater than the maximum ordinate of the k_p/k_r curve.

also intersect at a common point on the Z axis, the angle between the Z axis and the P axis for each element being $90^\circ - \phi$. Consequently, the Q principal elastic axes are each tangent to the circle of radius a_r which bounds the end face of the cylinder.

The use of such a configuration permits decoupling of all six modes of vibration of the rigid body. This complete decoupling is achieved if the angle of inclination ϕ has the value ϕ' which satisfies the following equation:

$$\left| \frac{a_z}{a_r} \right| = \frac{(\frac{1}{2})[1 - (k_p/k_r)] \sin 2\phi'}{(k_q/k_r) + (k_p/k_r) + [1 - (k_p/k_r)] \sin^2\phi'} \tag{3.50}$$

Since complete decoupling is effected, the system may be termed an “equivalent center-of-gravity system.”^{9,10} The natural frequencies of the six decoupled modes are

$$\frac{f_x}{f_r} = \frac{f_y}{f_r} = \sqrt{\frac{1}{2} \left(\frac{k_p}{k_r} \cos^2 \phi' + \sin^2 \phi' + \frac{k_q}{k_r} \right)} \tag{3.51}$$

$$\frac{f_\alpha}{f_r} = \frac{f_\beta}{f_r} = \left\{ \frac{a_r}{2\rho_x} \left[\frac{k_p}{k_r} \sin \phi' \left(\frac{a_r}{\rho_x} \sin \phi' + \frac{a_z}{\rho_x} \cos \phi' \right) + \cos \phi' \left(\frac{a_r}{\rho_x} \cos \phi' - \frac{a_z}{\rho_x} \sin \phi' \right) \right] \right\}^{1/2} \tag{3.52}$$

$$\frac{f_\gamma}{f_r} = \sqrt{\frac{k_q}{k_r} \frac{a_r}{\rho_z}} \tag{3.53}$$

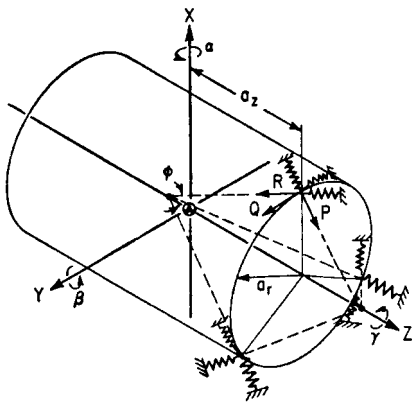


FIGURE 3.24 Example of a rigid cylindrical body on radially inclined resilient supports. The resilient supports are attached symmetrically about the Z axis to one end face of the cylinder at a distance a_r from the Z axis and a distance a_z from the XY plane. The resilient elements are inclined so that their principal elastic axes R and P intersect the Z axis at common points. The angle between the R axes and the Z axis is ϕ ; and the angle between the P axis and Z axis is $90^\circ - \phi$. The Q principal elastic axes are each tangent to the circle of radius a_r .

The frequency ratio f_z/f_r is given by Eq. (3.43) or Fig. 3.22. The fictitious natural frequency f_r is given by

$$f_r = (1/2\pi)\sqrt{nk_r/m}$$

Similar solutions are also available for the configuration of four resilient supports located in a rectangular array and inclined to achieve complete decoupling.¹¹

FORCED VIBRATION

Forced vibration results from a continuing excitation that varies sinusoidally with time. The excitation may be a vibratory displacement of the foundation for the resiliently supported rigid body (*foundation-induced vibration*), or a force or moment applied to or generated within the rigid body (*body-induced vibration*). These two forms of excitation are considered separately.

FOUNDATION-INDUCED SINUSOIDAL VIBRATION

This section includes an analysis of foundation-induced vibration for two different systems, each having two planes of symmetry. In one system, the principal elastic axes of the resilient elements are parallel to the X, Y, Z axes; in the other system, the principal elastic axes are inclined with respect to two of the axes but in a plane parallel to one of the reference planes. The excitation is translational movement of the foundation in its own plane, without rotation. No forces or moments are applied

directly to the rigid body; i.e., in the equations of motion [Eqs. (3.31)], the following terms are equal to zero:

$$F_x = F_y = F_z = M_x = M_y = M_z = \alpha = \beta = \gamma = 0 \tag{3.54}$$

Two Planes of Symmetry with Orthogonal Resilient Supports. The system is shown in Fig. 3.15. The excitation is a motion of the foundation in the direction of the X axis defined by $u = u_0 \sin \omega t$. (Alternatively, the excitation may be the displacement $v = v_0 \sin \omega t$ in the direction of the Y axis, and analogous results are obtained.) The resulting motion of the resiliently supported rigid body involves translation x_c and rotation β simultaneously. The conditions of symmetry are defined by Eqs. (3.33), (3.34), (3.35), and (3.38); these conditions decouple Eqs. (3.31) so that only Eqs. (3.31a) and (3.31d), and Eqs. (3.31b) and (3.31c), remain coupled. Upon substituting $u = u_0 \sin \omega t$ as the excitation, the response in the coupled modes is of a form $x_c = x_{c0} \sin \omega t$, $\beta = \beta_0 \sin \omega t$ where x_{c0} and β_0 are related to u_0 as follows:

$$\frac{x_{c0}}{u_0} = \frac{\frac{k_x}{k_z} \left[\left(\frac{a_x}{\rho_y} \right)^2 - \left(\frac{f}{f_z} \right)^2 \right]}{\left(\frac{f}{f_z} \right)^4 - \left[\frac{k_x}{k_z} + \frac{k_x}{k_z} \left(\frac{a_z}{\rho_y} \right)^2 + \left(\frac{a_x}{\rho_y} \right)^2 \right] \left(\frac{f}{f_z} \right)^2 + \frac{k_x}{k_z} \left(\frac{a_x}{\rho_y} \right)^2} \tag{3.55}$$

$$\frac{\beta_0}{u_0/\rho_y} = \frac{-\frac{k_x}{k_z} \frac{a_z}{\rho_y} \left(\frac{f}{f_z} \right)^2}{\left(\frac{f}{f_z} \right)^4 - \left[\frac{k_x}{k_z} + \frac{k_x}{k_z} \left(\frac{a_z}{\rho_y} \right)^2 + \left(\frac{a_x}{\rho_y} \right)^2 \right] \left(\frac{f}{f_z} \right)^2 + \frac{k_x}{k_z} \left(\frac{a_x}{\rho_y} \right)^2} \tag{3.56}$$

where $f_z = \frac{1}{2\pi} \sqrt{4k_z/m}$ in accordance with Eq. (3.37). A similar set of equations apply for vibration in the coupled y_c , α coordinates. There is no response of the system in the z_c or γ modes since there is no net excitation in these directions; that is, F_z and M_z are zero.

As indicated by Eqs. (3.1), the displacement at any point in a rigid body is the sum of the displacement at the center-of-gravity and the displacements resulting from motion of the body in rotation about axes through the center-of-gravity. Equations

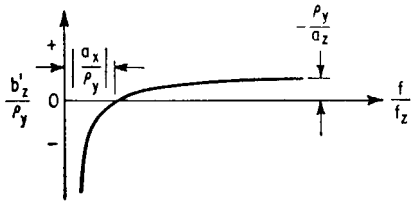


FIGURE 3.25 Curve showing the position of the axis of pure rotation of the rigid body in Fig. 3.15 as a function of the frequency ratio f/f_z when the excitation is sinusoidal motion of the foundation in the X direction [see Eq. (3.57)]. The axis of rotation is parallel to the Y axis and in the XZ plane, and its coordinate along the Z axis is designated by b'_z .

(3.55) and (3.56) together with analogous equations for y_{c0} , α_0 provide the basis for calculating these displacements. Care should be taken with phase angles, particularly if two or more excitations u , v , w exist concurrently.

At any single frequency, coupled vibration in the x_c , β modes is equivalent to a pure rotation of the rigid body with respect to an axis parallel to the Y axis, in the YZ plane and displaced from the center-of-gravity of the body (see Fig. 3.15). As a result, the rigid body has zero displacement x in the horizontal plane containing this axis. Therefore, the Z coordinate of this axis b'_z satisfies $x_{c0} + b'_z \beta_0 = 0$, which is obtained from the first

of Eqs. (3.1) by setting $x_b = 0$ (γ_0 motion is not considered). Substituting Eqs. (3.55) and (3.56) for x_{c0} and β_0 , respectively, the axis of rotation is located at

$$\frac{b'_z}{\rho_y} = \frac{(a_x/\rho_y)^2 - (f/f_z)^2}{(a_z/\rho_y)(f/f_z)^2} \tag{3.57}$$

Figure 3.25 shows the relation of Eq. (3.57) graphically. At high values of frequency f/f_z , the axis does not change position significantly with frequency; b'_z/ρ_y approaches a positive value as f/f_z becomes large, since a_z is negative (see Fig. 3.15).

When the resilient supporting elements have damping as well as elastic properties, the solution of the equations of motion [see Eq. (3.31a)] becomes too laborious for general use. Responses of systems with damping have been obtained for several typical cases using a digital computer. Figures 3.26 A, B, and C show the response at three points in the body of the system shown in Fig. 3.15, with the excitation $u = u_0 \sin \omega t$. The weight of the body is 45 lb; each of the four resilient supporting elements has a stiffness $k_z = 1,050$ lb/in. and stiffness ratios $k_x/k_z = k_y/k_z = 1/2$. The critical damping coefficients in the X, Y, Z directions are taken as $c_{cx} = 2\sqrt{4k_x m}$, $c_{cy} = 2\sqrt{4k_y m}$, $c_{cz} = 2\sqrt{4k_z m}$, respectively, where the expression for c_{cz} follows from the single degree-of-freedom case defined by Eq. (2.12). The fractions of critical damping are $c_x/c_{cx} =$

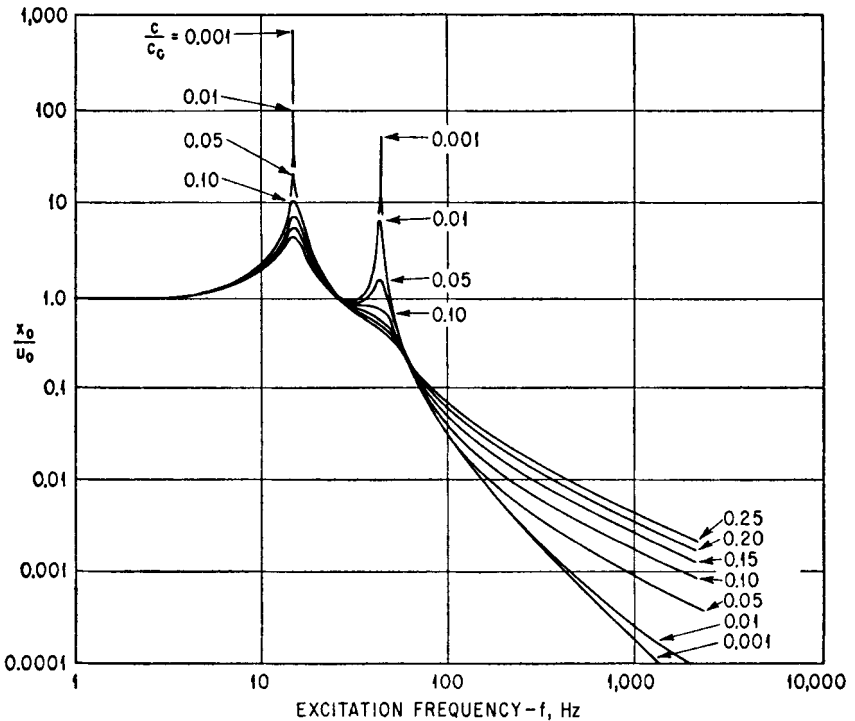


FIGURE 3.26A Response curves for point 1 with damping in the resilient supports in the system shown in Fig. 3.15. The response is the ratio of the amplitude at point 1 of the rigid body in the X direction to the amplitude of the foundation in the X direction (x_0/u_0). The fraction of critical damping c/c_c is the same in the X, Y, Z directions.

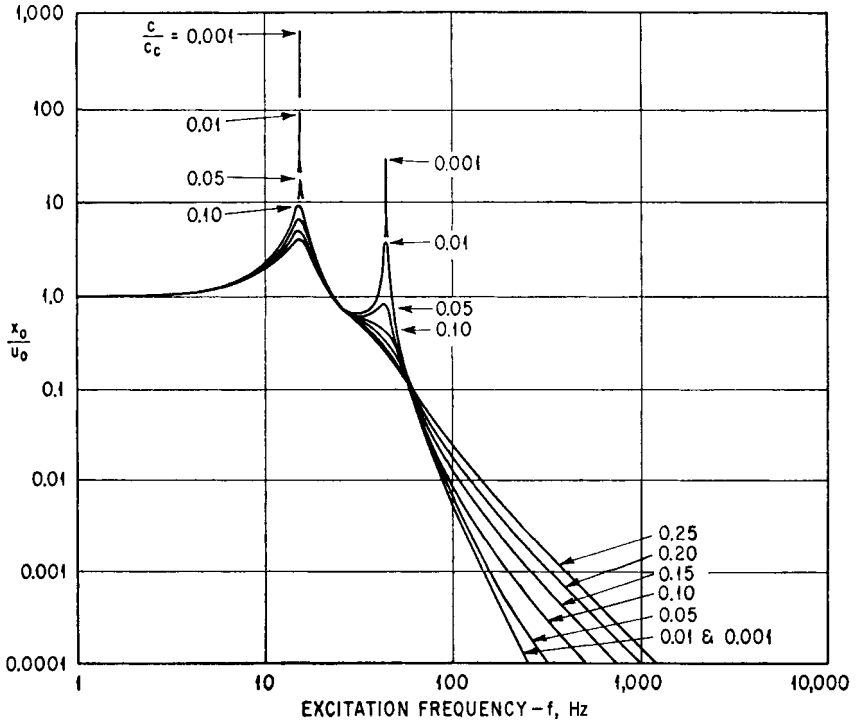


FIGURE 3.26B Response curves at point 2 in the system shown in Fig. 3.15. See caption for Fig. 3.26A.

$c_y/c_{cy} = c_z/c_{cz} = c/c_c$, the parameter of the curves in Figs. 3.26A, B, and C. Coordinates locating the resilient elements are $a_x = \pm 5.25$ in., $a_y = \pm 3.50$ in., and $a_z = -6.50$ in. The radii of gyration with respect to the X, Y, Z axes are $\rho_x = 4.40$ in., $\rho_y = 5.10$ in., and $\rho_z = 4.60$ in.

Natural frequencies calculated from Eqs. (3.37) and (3.40) are $f_z = 30.0$ Hz; $f_{xB} = 43.7$ Hz, 15.0 Hz; and $f_{y\alpha} = 43.2$ Hz, 11.7 Hz. The fraction of critical damping c/c_c varies between 0 and 0.25. Certain characteristic features of the response curves in Figs. 3.26A, B, and C are:

1. The relatively small response at the frequency of 24.2 Hz in Fig. 3.26C occurs because point 3 lies near the axis of rotation of the rigid body at that frequency. Point 2 lies near the axis of rotation at higher frequencies, and the response becomes correspondingly low, as shown in Fig. 3.26B. The position of the axis of rotation changes rapidly for small changes of frequency in the low- and intermediate-frequency range (indicated by the sharp dip in the curves for small damping in Fig. 3.26C) and varies asymptotically toward a final position as the forcing frequency increases (see Fig. 3.25).

2. The effect of damping on the magnitude of the response at the higher and lower natural frequencies in coupled modes is illustrated. When the fraction of critical damping is between 0.01 and 0.10, the response at the lower of the coupled nat-

ural frequencies is approximately 10 times as great as the response at the higher of the coupled natural frequencies. With greater damping ($c/c_c \geq 0.15$), the effect of resonance in the vicinity of the higher coupled natural frequency becomes so slight as to be hardly discernible.

Two Planes of Symmetry with Resilient Supports Inclined in One Plane Only.

The system is shown in Fig. 3.21, and the excitation is $u = u_0 \sin \omega t$. The conditions of symmetry are defined by Eqs. (3.33), (3.35), and (3.38). The response is entirely in the x_c, β coupled mode with the following amplitudes:

$$\begin{aligned} \frac{x_{c0}}{u_0} &= \frac{\frac{k_p}{k_r} \left(\frac{a_x}{\rho_y} \right)^2 - \left(\frac{k_p}{k_r} \cos^2 \phi + \sin^2 \phi \right) \left(\frac{f}{f_r} \right)^2}{\left(\frac{f}{f_r} \right)^4 - A \left(\frac{f}{f_r} \right)^2 + \frac{k_p}{k_r} \left(\frac{a_x}{\rho_y} \right)^2} \\ \frac{\beta_0}{u_0/\rho_y} &= \frac{- \left[\left(\frac{k_p}{k_r} \cos^2 \phi + \sin^2 \phi \right) \left(\frac{a_z}{\rho_y} \right) + \left(1 - \frac{k_p}{k_r} \right) \left| \frac{a_x}{\rho_y} \right| \sin \phi \cos \phi \right] \left(\frac{f}{f_r} \right)^2}{\left(\frac{f}{f_r} \right)^4 - A \left(\frac{f}{f_r} \right)^2 + \frac{k_p}{k_r} \left(\frac{a_x}{\rho_y} \right)^2} \end{aligned} \quad (3.58)$$

where A is defined after Eq. (3.45). A similar set of expressions may be written for the response in the y_c, α coupled mode when the excitation is the motion $v = v_0 \sin \omega t$ of the foundation:

$$\begin{aligned} \frac{y_{c0}}{v_0} &= \frac{\frac{k_q}{k_r} \left(\frac{k_p}{k_r} \sin^2 \phi + \cos^2 \phi \right) \left(\frac{a_y}{\rho_x} \right)^2 - \frac{k_q}{k_r} \left(\frac{f}{f_r} \right)^2}{\left(\frac{f}{f_r} \right)^4 - B \left(\frac{f}{f_r} \right)^2 + \frac{k_q}{k_r} \left(\frac{k_p}{k_r} \sin^2 \phi + \cos^2 \phi \right) \left(\frac{a_y}{\rho_x} \right)^2} \\ \frac{\alpha_0}{v_0/\rho_x} &= \frac{\frac{k_q}{k_r} \frac{a_z}{\rho_x} \left(\frac{f}{f_r} \right)^2}{\left(\frac{f}{f_r} \right)^4 - B \left(\frac{f}{f_r} \right)^2 + \frac{k_q}{k_r} \left(\frac{k_p}{k_r} \sin^2 \phi + \cos^2 \phi \right) \left(\frac{a_y}{\rho_x} \right)^2} \end{aligned} \quad (3.59)$$

where B is defined after Eq. (3.46). No motion occurs in the z_c or γ mode since the quantities F_z and M_z are zero in Eqs. (3.31e) and (3.31f).

Response curves for the system shown in Fig. 3.21 when damping is included are qualitatively similar to those shown in Figs. 3.26. The significant advantage in the use of inclined resilient supports is the additional versatility gained from the ability to vary the angle of inclination ϕ , which directly affects the degree of coupling in the x_c, β coupled mode. For example, a change in the angle ϕ produces a change in the position of the axis of pure rotation of the rigid body. In a manner similar to that used to derive Eq. (3.57), Eqs. (3.58) yield the following expression defining the location of the axis of rotation:

$$\frac{b'_z}{\rho_y} = \frac{\frac{k_p}{k_r} \left(\frac{a_x}{\rho_y} \right)^2 - \left(\frac{k_p}{k_r} \cos^2 \phi + \sin^2 \phi \right) \left(\frac{f}{f_r} \right)^2}{\left[\left(\frac{k_p}{k_r} \cos^2 \phi + \sin^2 \phi \right) \frac{a_z}{\rho_y} + \left(1 - \frac{k_p}{k_r} \right) \left| \frac{a_x}{\rho_y} \right| \sin \phi \cos \phi \right] \left(\frac{f}{f_r} \right)^2} \quad (3.60)$$

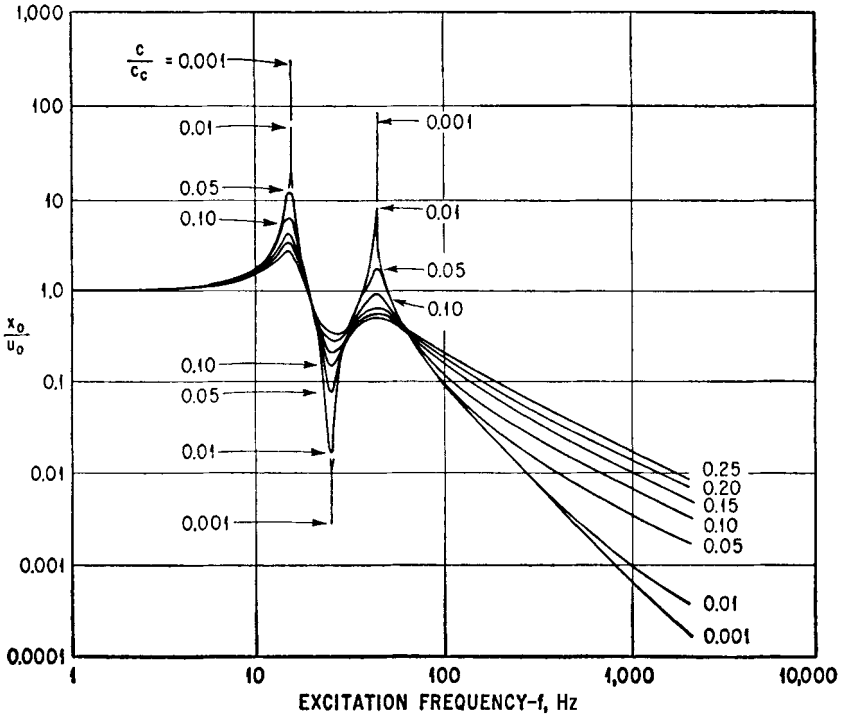


FIGURE 3.26C Response curves at point 3 in the system shown in Fig. 3.15. See caption for Fig. 3.26A.

BODY-INDUCED SINUSOIDAL VIBRATION

This section includes the analysis of a resiliently supported rigid body wherein the excitation consists of forces and moments applied directly to the rigid body (or originating within the body). The system has two planes of symmetry with orthogonal resilient supports; the modal coupling and natural frequencies for such a system are considered above. Two types of excitation are considered: (1) a force rotating about an axis parallel to one of the principal inertial axes and (2) an oscillatory moment acting about one of the principal inertial axes. There is no motion of the foundation that supports the resilient elements; thus, the following terms in Eqs. (3.31) are equal to zero:

$$u = v = w = \alpha = \beta = \gamma = 0 \tag{3.61}$$

Two Planes of Symmetry with Orthogonal Resilient Elements Excited by a Rotating Force. The system excited by the rotating force is illustrated in Fig. 3.27. The force F_0 rotates at frequency ω about an axis parallel to the Y axis but spaced therefrom by the coordinate distances d_x, d_z ; the force is in the XZ plane. The forces and moments applied to the body by the rotating force F_0 are

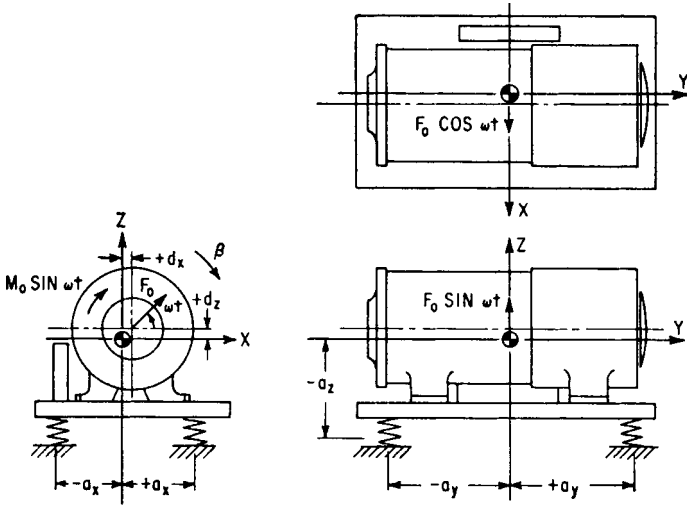


FIGURE 3.27 Example of a rigid body on orthogonal resilient supports with two planes of symmetry, excited by body-induced sinusoidal excitation. Alternative excitations are (1) the force F_0 in the XZ plane rotating with angular velocity ωt about an axis parallel to the Y axis and (2) the oscillatory moment $M_0 \sin \omega t$ acting about the Y axis. There is no motion of the foundation that supports the resilient elements.

$$\begin{aligned}
 F_x &= F_0 \cos \omega t & M_x &= 0 \\
 F_y &= 0 & M_y &= F_0(d_z \cos \omega t - d_x \sin \omega t) \\
 F_z &= F_0 \sin \omega t & M_z &= 0
 \end{aligned}
 \tag{3.62}$$

The conditions of symmetry are defined by Eqs. (3.33), (3.34), (3.35), and (3.38); and the excitation is defined by Eqs. (3.61) and (3.62). Substituting these conditions into the equations of motion, Eqs. (3.31) show that vibration response is not excited in the coupled y_c , α mode or in the γ mode. In the Z direction, the motion z_{c0} of the body and the force F_{tz} transmitted through the resilient elements can be found from Eq. (2.30) and Fig. 2.17 since single degree-of-freedom behavior is involved. The horizontal displacement amplitude x_{c0} of the center-of-gravity in the X direction and the rotational displacement amplitude β_0 about the Y axis are given by

$$\begin{aligned}
 \frac{x_{c0}}{F_0/4k_x} &= \frac{k_x}{k_z} \sqrt{\left[\frac{k_x}{k_z} \frac{a_z}{\rho_y} \left(\frac{a_z}{\rho_y} - \frac{d_z}{\rho_y} \right) + \left(\frac{a_x}{\rho_y} \right)^2 - \left(\frac{f}{f_z} \right)^2 \right]^2 + \left[\frac{k_x}{k_z} \frac{d_x}{\rho_y} \frac{a_z}{\rho_y} \right]^2} \\
 &\quad \frac{1}{\left(\frac{f}{f_z} \right)^4 - \left[\frac{k_x}{k_z} + \frac{k_x}{k_z} \left(\frac{a_z}{\rho_y} \right)^2 + \left(\frac{a_x}{\rho_y} \right)^2 \right] \left(\frac{f}{f_z} \right)^2 + \frac{k_x}{k_z} \left(\frac{a_x}{\rho_y} \right)^2} \\
 \beta_0 &= \frac{k_x}{F_0/4k_x \rho_y} \sqrt{\left[\frac{k_x}{k_z} \left(\frac{a_z}{\rho_y} - \frac{d_z}{\rho_y} \right) + \frac{d_z}{\rho_y} \left(\frac{f}{f_z} \right)^2 \right]^2 + \left[\frac{d_x}{\rho_y} \left(\frac{k_x}{k_z} - \frac{f^2}{f_z^2} \right) \right]^2} \\
 &\quad \frac{1}{\left(\frac{f}{f_z} \right)^4 - \left[\frac{k_x}{k_z} + \frac{k_x}{k_z} \left(\frac{a_z}{\rho_y} \right)^2 + \left(\frac{a_x}{\rho_y} \right)^2 \right] \left(\frac{f}{f_z} \right)^2 + \frac{k_x}{k_z} \left(\frac{a_x}{\rho_y} \right)^2}
 \end{aligned}
 \tag{3.63}$$

where a_x, a_z are location coordinates of the resilient supports, and

$$f_z = \frac{1}{2\pi} \sqrt{\frac{4k_z}{m}} \tag{3.64}$$

The amplitude of the oscillating force F_{tx} in the X direction and the amplitude of the oscillating moment M_{ty} about the Y axis which are transmitted to the foundation by the combination of resilient elements are

$$\begin{aligned} F_{tx} &= 4k_x \sqrt{x_{c0}^2 - 2a_z x_{c0} \beta_0 \cos(\phi_x - \phi_\beta) + a_z^2 \beta_0^2} \\ M_{ty} &= 4k_z a_x^2 \beta_0 \end{aligned} \tag{3.65}$$

where F_{tx} is the sum of the forces transmitted by the individual resilient elements and M_{ty} is a moment formed by forces in the Z direction of opposite sign at opposite resilient supports. The angles ϕ_x and ϕ_β are defined by

$$\begin{aligned} \tan \phi_x &= \frac{\frac{k_x}{k_z} \frac{a_z}{\rho_y} \left(\frac{a_z}{\rho_y} - \frac{d_z}{\rho_y} \right) + \left(\frac{a_x}{\rho_y} \right)^2 - \left(\frac{f}{f_z} \right)^2}{\frac{k_x}{k_z} \frac{a_z}{\rho_y} \frac{d_x}{\rho_y}} \quad [0^\circ \leq \phi_x \leq 360^\circ] \\ \tan \phi_\beta &= \frac{\frac{k_x}{k_z} \left(\frac{a_z}{\rho_y} - \frac{d_z}{\rho_y} \right) + \frac{d_z}{\rho_y} \left(\frac{f}{f_z} \right)^2}{\frac{d_x}{\rho_y} \left[\frac{k_x}{k_z} - \left(\frac{f}{f_z} \right)^2 \right]} \quad [0^\circ \leq \phi_\beta \leq 360^\circ] \end{aligned}$$

To obtain the correct value of $(\phi_x - \phi_\beta)$ in Eq. (3.65), the signs of the numerator and denominator in each tangent term must be inspected to determine the proper quadrant for ϕ_x and ϕ_β .

Example 3.2. Consider an electric motor which has an unbalanced rotor, creating a centrifugal force. The motor weighs 3,750 lb, and has a radius of gyration $\rho_y = 9.10$ in. The distances $d_x = d_y = d_z = 0$, that is, the axis of rotation is the Y principal axis and the center-of-gravity of the rotor is in the XZ plane. The resilient supports each have a stiffness ratio of $k_x/k_z = 1.16$, and are located at $a_z = -14.75$ in., $a_x = \pm 12.00$ in. The resulting displacement amplitudes of the center-of-gravity, expressed dimensionlessly, are shown in Fig. 3.28; the force and moment amplitudes transmitted to the foundation, expressed dimensionlessly, are shown in Fig. 3.29. The displacements of the center-of-gravity of the body are dimensionalized with respect to the displacements at zero frequency:

$$\begin{aligned} z_{c0}(0) &= \frac{F_0}{4k_z} \\ x_{c0}(0) &= \frac{F_0}{4k_x} \left[1 + \frac{k_x}{k_z} \left(\frac{a_z}{a_x} \right)^2 \right] \\ \beta_0(0) &= \frac{F_0}{4k_z a_z} \left(\frac{a_z}{a_x} \right)^2 \end{aligned} \tag{3.66}$$

At excitation frequencies greater than the higher natural frequency of the x_c, β coupled motion, the displacements, forces, and moment all continuously decrease as the frequency increases.

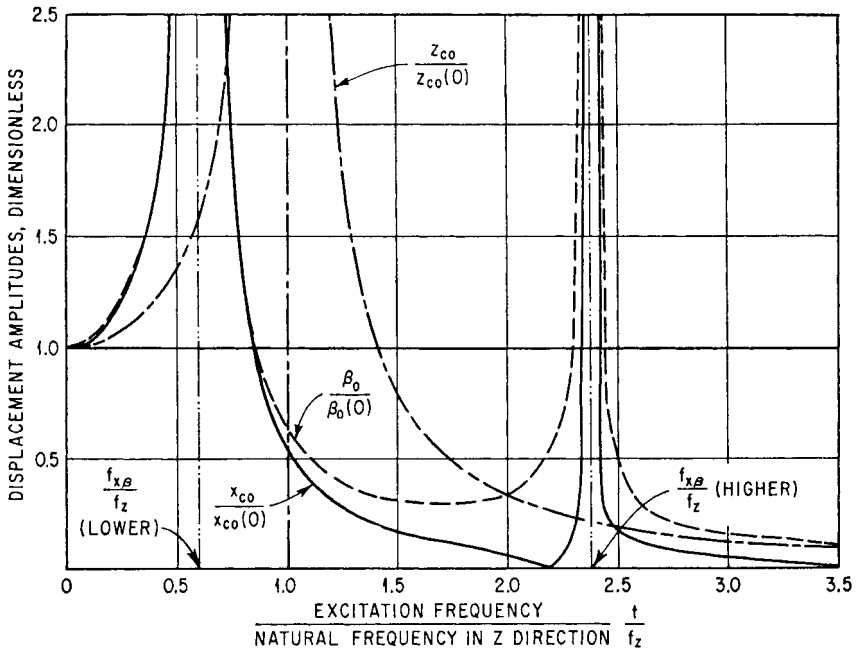


FIGURE 3.28 Response curves for the system shown in Fig. 3.27 when excited by a rotating force F_0 acting about the Y axis. The parameters of the system are $k_x/k_z = 1.16$, $a_x/\rho_y = \pm 1.32$, $a_z/\rho_y = -1.62$. Only x_c, z_c, β displacements of the body are excited [see Eqs. (3.63)]. The displacements are expressed dimensionlessly by employing the displacements at zero frequency [see Eqs. (3.66)].

Two Planes of Symmetry with Orthogonal Resilient Elements Excited by an Oscillating Moment. Consider the oscillatory moment M_0 acting about the Y axis with forcing frequency ω . The resulting applied forces and moments acting on the body are

$$\begin{aligned}
 M_y &= M_0 \sin \omega t \\
 F_x &= F_y = F_z = M_x = M_z = 0
 \end{aligned}
 \tag{3.67}$$

Substituting conditions of symmetry defined by Eqs. (3.33), (3.34), (3.35), and (3.38), and the excitation defined by Eqs. (3.61) and (3.67), the equations of motion [Eqs. (3.31)] show that oscillations are excited only in the x_c, β coupled mode. Solving for the resulting displacements,

$$\begin{aligned}
 \frac{x_{c0}}{M_0/4k_x\rho_y} &= \frac{\left(\frac{k_x}{k_z}\right)^2 \frac{a_z}{\rho_y}}{\left(\frac{f}{f_z}\right)^4 - \left[\frac{k_x}{k_z} + \frac{k_x}{k_z} \left(\frac{a_z}{\rho_y}\right)^2 + \left(\frac{a_x}{\rho_y}\right)^2\right] \left(\frac{f}{f_z}\right)^2 + \frac{k_x}{k_z} \left(\frac{a_x}{\rho_y}\right)^2} \\
 \beta_0 &= \frac{\frac{k_x}{k_z} \left[\frac{k_x}{k_z} - \left(\frac{f}{f_z}\right)^2\right]}{\left(\frac{f}{f_z}\right)^4 - \left[\frac{k_x}{k_z} + \frac{k_x}{k_z} \left(\frac{a_z}{\rho_y}\right)^2 + \left(\frac{a_x}{\rho_y}\right)^2\right] \left(\frac{f}{f_z}\right)^2 + \frac{k_x}{k_z} \left(\frac{a_x}{\rho_y}\right)^2}
 \end{aligned}
 \tag{3.68}$$

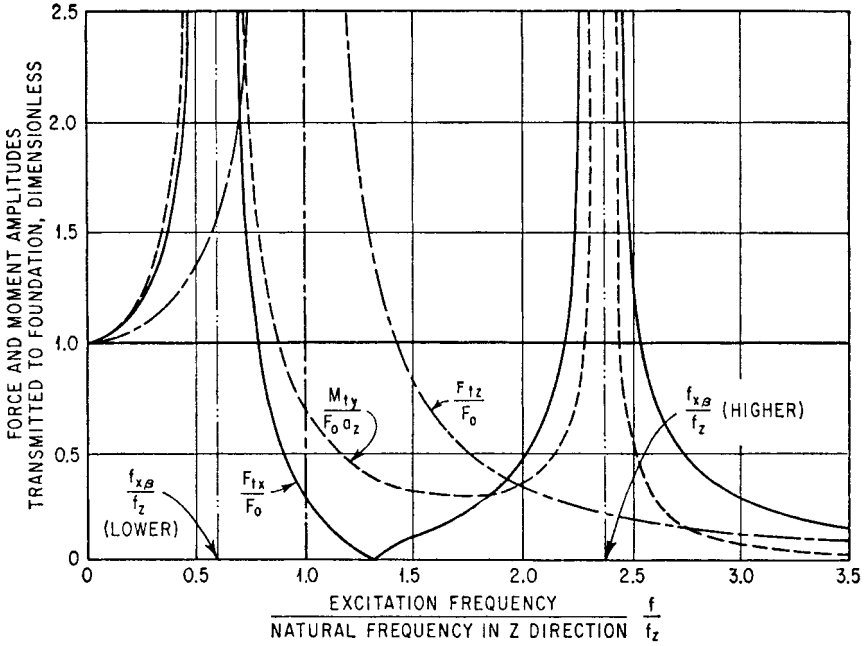


FIGURE 3.29 Force and moment amplitudes transmitted to the foundation for the system shown in Fig. 3.27 when excited by a rotating force F_0 acting about the Y axis. The parameters of the system are $k_x/k_z = 1.16$, $a_x/\rho_y = \pm 1.32$, $a_z/\rho_y = -1.62$. The amplitudes of the oscillating forces in the X and Z directions transmitted to the foundation are F_{tx} and F_{tz} , respectively. The amplitude of the total oscillating moment about the Y axis transmitted to the foundation is M_{ty} .

The amplitude of the oscillating force F_{tx} in the X direction and the amplitude of the oscillating moment M_{ty} about the Y axis transmitted to the foundation by the combination of resilient supports are

$$\begin{aligned}
 F_{tx} &= 4k_x(x_{c0} - a_z\beta_0) \\
 M_{ty} &= 4k_z a_x^2 \beta_0
 \end{aligned}
 \tag{3.69}$$

where F_{tx} and M_{ty} have the same meaning as in Eqs. (3.65). Low vibration transmission of force and moment to the foundation is decreased at the higher frequencies in a manner similar to that shown in Fig. 3.29.

FOUNDATION-INDUCED VELOCITY SHOCK

A velocity shock is an instantaneous change in the velocity of one portion of a system relative to another portion. In this section, the system is a rigid body supported by orthogonal resilient elements within a rigid container; the container experiences a velocity shock. The system has one plane of symmetry; modal coupling and natural frequencies for such a system are considered above. Two types of velocity shock are analyzed: (1) a sudden change in the translational velocity of the container and (2) a sudden change in the rotational velocity of the container. In both instances the change in velocity is from an initial velocity to zero. No forces or moments are

applied directly to the resiliently supported body; i.e., only the forces transmitted by the resilient supports act. Thus, in the equations of motion, Eqs. (3.31):

$$F_x = F_y = F_z = M_x = M_y = M_z = 0 \quad (3.70)$$

The modal coupling and natural frequencies for this system have been determined when the YZ plane is a plane of symmetry and the conditions of symmetry of Eqs. (3.33) to (3.35) apply. It is assumed that the velocity components of the body ($\dot{x}_c, \dot{y}_c, \dot{z}_c, \dot{\alpha}, \dot{\beta}, \dot{\gamma}$) and the velocity components of the supporting container ($\dot{u}, \dot{v}, \dot{w}, \dot{\alpha}, \dot{\beta}, \dot{\gamma}$) are respectively equal at time $t < 0$. At $t = 0$, all velocity components of the supporting container are brought to zero instantaneously. To determine the subsequent motion of the resiliently supported body, the natural frequencies f_n in the coupled modes of response are first calculated using Eq. (3.36). Then the response motion of the resiliently supported body to the two types of velocity shock can be found by the analyses which follow.

One Plane of Symmetry with Orthogonal Resilient Supports Excited by a Translational Velocity Shock. Figure 3.30 shows a rigid body supported within a rigid container by resilient supports in such a manner that the YZ plane is a plane of symmetry. The entire system moves with constant velocity \dot{v}_0 and without relative motion. At time $t = 0$, the container impacts inelastically against the rigid wall shown at the right. The following initial conditions of displacement and velocity apply at the instant of impact ($t = 0$):

$$\begin{aligned} \dot{y}_c(0) &= \dot{v}_0 \\ x_c(0) &= y_c(0) = z_c(0) = \alpha(0) = \beta(0) = \gamma(0) = 0 \\ \dot{x}_c(0) &= \dot{z}_c(0) = \dot{\alpha}(0) = \dot{\beta}(0) = \dot{\gamma}(0) = 0 \end{aligned} \quad (3.71)$$

As a result of the impact, the velocity of the supported rigid body tends to continue and is responsible for excitation of the system in the coupled mode of the y_c, z_c, α motions. The maximum displacements of the center-of-gravity of the supported body are

$$\begin{aligned} \frac{y_{cm}}{2\pi\dot{v}_0/f_z} &= \frac{1}{B} \sum_{n=1}^3 \left(\frac{|A_n|}{f_n/f_z} \right) \\ \frac{z_{cm}}{2\pi\dot{v}_0/f_z} &= \frac{1}{B} \sum_{n=1}^3 \left(\frac{|M_n A_n|}{f_n/f_z} \right) \\ \frac{\alpha_m}{2\pi\dot{v}_0/\rho_x f_z} &= \frac{1}{B} \sum_{n=1}^3 \left(\frac{|N_n A_n|}{f_n/f_z} \right) \end{aligned} \quad (3.72)$$

The maximum accelerations of the center-of-gravity of the supported body are

$$\begin{aligned} \frac{\ddot{y}_{cm}}{2\pi f_z \dot{v}_0} &= \frac{1}{B} \sum_{n=1}^3 \left(|A_n| \frac{f_n}{f_z} \right) \\ \frac{\ddot{z}_{cm}}{2\pi f_z \dot{v}_0} &= \frac{1}{B} \sum_{n=1}^3 \left(|M_n A_n| \frac{f_n}{f_z} \right) \\ \frac{\ddot{\alpha}_m}{2\pi f_z \dot{v}_0/\rho_x} &= \frac{1}{B} \sum_{n=1}^3 \left(|N_n A_n| \frac{f_n}{f_z} \right) \end{aligned} \quad (3.73)$$

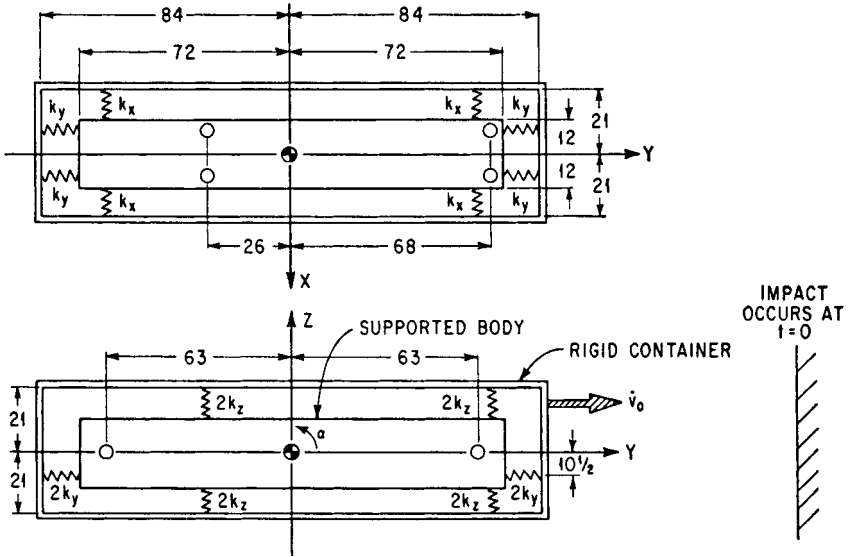


FIGURE 3.30 Example of a rigid body supported within a rigid container by resilient elements with YZ a plane of symmetry. Excitation is by a translational velocity shock in the Y direction. Prior to impact the entire system moves with constant velocity \dot{v}_0 and without relative motion. The rigid container impacts inelastically against the wall shown at the right, and y_c, z_c, α motions of the internally supported body result, as described mathematically by Eqs. (3.72) and (3.73).

where the subscript m denotes maximum value and

$$\begin{aligned}
 M_n &= \frac{1}{1 - (f_n/f_z)^2} \left[\frac{\Sigma k_y}{\Sigma k_z} - \left(\frac{f_n}{f_z} \right)^2 \right] \frac{\Sigma k_z a_y}{\Sigma k_y a_z} \\
 N_n &= \left[\frac{\Sigma k_y}{\Sigma k_z} - \left(\frac{f_n}{f_z} \right)^2 \right] \frac{\rho_x \Sigma k_z}{\Sigma k_y a_z} \\
 A_n &= M_{n+1} N_{n+2} - M_{n+2} N_{n+1} \\
 B &= \left| \sum_{n=1}^3 M_n (N_{n+1} - N_{n+2}) \right|
 \end{aligned}
 \tag{3.74}$$

The fictitious natural frequency f_z is defined for mathematical purposes by Eq. (3.37). The numerical values of the subscript numbers $n, n+1, n+2$ denote the three natural frequencies in the coupled mode of the y_c, z_c, α motions determined from Eq. (3.36). These natural frequencies are arbitrarily assigned the values $n = 1, 2, 3$. When $n+1$ or $n+2$ equals 4, use 1 instead; when $n+2$ equals 5, use 2 instead. Maximum displacements and accelerations may be calculated for other points in the supported rigid body by using Eqs. (3.1) except that each of the terms must be made numerically additive. For example, the maximum value of the y displacement at the point b having the Z coordinate b_z is

$$y_{bm} = y_{cm} + |b_z| \alpha_m
 \tag{3.75}$$

since $\gamma = 0$.

Since the system is assumed undamped, the response of the suspended body in terms of displacement or acceleration consists of a superposition of three sinusoidal components at the three natural frequencies in the coupled y_c , z_c , α mode. The absolute values of terms appear in Eq. (3.75) because the maximum response is the sum of the amplitudes of the three component vibrations which make up the over-all response. In general, the maximum response occurs when the three component vibrations reach their maximum positive or negative values at the same instant. Thus, the maximum values of response apply both in positive and negative directions.

One Plane of Symmetry with Orthogonal Resilient Supports Excited by a Rotational Velocity Shock. Alternative to the type of impact illustrated in Fig. 3.30, the system may be excited by imparting a rotational velocity shock (e.g., by lifting and dropping one end of the container), as illustrated in Fig. 3.31. It is assumed that the container impacts inelastically. The system has the same form of symmetry as that shown in Fig. 3.30, and only the y_c , z_c , α modes are excited. The initial conditions at the instant of impact ($t = 0$), based upon the angular velocity $\dot{\alpha}_0$ of the rigid container about point A in Fig. 3.31, are

$$\begin{aligned} \dot{y}_c(0) &= -d_z \dot{\alpha}_0 & \dot{z}_c(0) &= d_y \dot{\alpha}_0 & \dot{\alpha}(0) &= \dot{\alpha}_0 \\ x_c(0) &= y_c(0) = z_c(0) = \alpha(0) = \beta(0) = \gamma(0) = 0 \\ \dot{x}_c(0) &= \dot{\beta}(0) = \dot{\gamma}(0) = 0 \end{aligned} \quad (3.76)$$

Note that d_y and d_z are negative quantities. The initial conditions in Eqs. (3.76) are based on the assumption that motion of the rigid body relative to the container during the fall is negligible compared to that which occurs after the impact. The maximum displacements of the center-of-gravity of the supported body are

$$\begin{aligned} \frac{y_{cm}}{2\pi\rho_x \dot{\alpha}_0 f_z} &= \frac{1}{B} \sum_{n=1}^3 \left[\left| \frac{d_z}{\rho_x} A_n + \frac{d_y}{\rho_x} (N_{n+1} - N_{n+2}) + (M_{n+2} - M_{n+1}) \right| \frac{f_z}{f_n} \right] \\ \frac{z_{cm}}{2\pi\rho_x \dot{\alpha}_0 f_z} &= \frac{1}{B} \sum_{n=1}^3 \left[\left| M_n \left(\frac{d_z}{\rho_x} A_n + \frac{d_y}{\rho_x} (N_{n+1} - N_{n+2}) + (M_{n+2} - M_{n+1}) \right) \right| \frac{f_z}{f_n} \right] \\ \frac{\alpha_m}{2\pi \dot{\alpha}_0 f_z} &= \frac{1}{B} \sum_{n=1}^3 \left[\left| N_n \left(\frac{d_z}{\rho_x} A_n + \frac{d_y}{\rho_x} (N_{n+1} - N_{n+2}) + (M_{n+2} - M_{n+1}) \right) \right| \frac{f_z}{f_n} \right] \end{aligned} \quad (3.77)$$

The maximum accelerations of the center-of-gravity of the supported body are

$$\begin{aligned} \frac{\ddot{y}_{cm}}{2\pi\rho_x f_z \dot{\alpha}_0} &= \frac{1}{B} \sum_{n=1}^3 \left[\left| \frac{d_z}{\rho_x} A_n + \frac{d_y}{\rho_x} (N_{n+1} - N_{n+2}) + (M_{n+2} - M_{n+1}) \right| \frac{f_n}{f_z} \right] \\ \frac{\ddot{z}_{cm}}{2\pi\rho_x f_z \dot{\alpha}_0} &= \frac{1}{B} \sum_{n=1}^3 \left[\left| M_n \left(\frac{d_z}{\rho_x} A_n + \frac{d_y}{\rho_x} (N_{n+1} - N_{n+2}) + (M_{n+2} - M_{n+1}) \right) \right| \frac{f_n}{f_z} \right] \\ \frac{\ddot{\alpha}_m}{2\pi f_z \dot{\alpha}_0} &= \frac{1}{B} \sum_{n=1}^3 \left[\left| N_n \left(\frac{d_z}{\rho_x} A_n + \frac{d_y}{\rho_x} (N_{n+1} - N_{n+2}) + (M_{n+2} - M_{n+1}) \right) \right| \frac{f_n}{f_z} \right] \end{aligned} \quad (3.78)$$

where d_z and d_y are the Z and Y coordinates, respectively, of the edges of the container, as shown in Fig. 3.31, and the other quantities are the same as those appear-

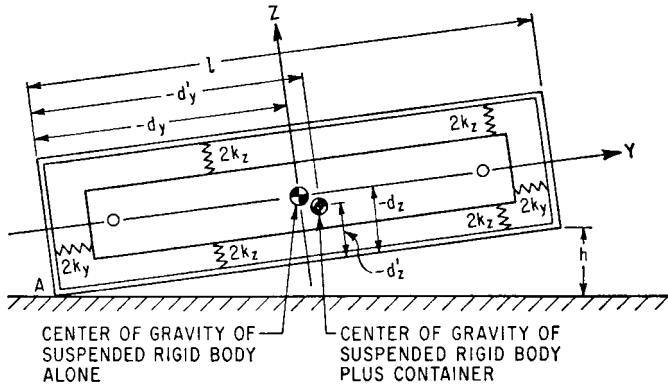


FIGURE 3.31 System shown in Fig. 3.30 excited by a rotational velocity shock about the X axis. The shock is induced by lifting and dropping one end of the rigid container to make inelastic impact with the foundation. If the height of drop is h , the rotational velocity of the system about the corner A at the instant of impact is given by Eq. (3.79). The response of the resiliently supported body is described mathematically by Eqs. (3.77) and (3.78).

ing in Eqs. (3.72) and (3.74). The maximum response at any point in the suspended body can be found in the manner of Eq. (3.75).

The rotational velocity $\dot{\alpha}_0$ of the container about the corner A in Fig. 3.31 may be induced by lifting the opposite end to a height h and dropping it. The resulting velocity $\dot{\alpha}_0$ is

$$\dot{\alpha}_0 = \left\{ \frac{2g}{\rho_A^2} \left[\frac{h}{l} d'_y + d'_z \sqrt{1 - \left(\frac{h}{l}\right)^2} - d'_z \right] \right\}^{1/2} \tag{3.79}$$

where g is the acceleration of gravity, ρ_A is the radius of gyration of the rigid body plus container about the corner A , h is the initial elevation of the raised end of the container, l is the length of the container, and d'_y and d'_z are the Y and Z coordinates, respectively, of the edges of the container with respect to the center-of-gravity of the assembly of rigid body plus container (see Fig. 3.31).

Example 3.3. The rigid body shown in Fig. 3.31 weighs 1,500 lb and has a radius of gyration $\rho_x = 42$ in. with respect to the X axis. The resilient supporting elements apply forces parallel to their longitudinal axes *only*. Each element with its longitudinal axis in the X or Y direction has a stiffness of $k_x = k_y = 500$ lb/in. Each element whose longitudinal axis extends in the Z direction has a stiffness $k_z = 1,000$ lb/in. The resilient elements are positioned as shown in Fig. 3.30, and $l = 168$ in., $d_y = d'_y = -84$ in., $d_z = d'_z = -21$ in., $\rho_A = 308$ in. The rotational velocity shock results from a height of drop $h = 36$ in.

The fictitious natural frequency f_z is obtained from Eq. (3.37), yielding $f_z = 7.22$ Hz. From Eq. (3.36) or Fig. 3.14, the natural frequencies in the y_c, z_c, α mode are $f_1 = 3.58$ Hz, $f_2 = 6.02$ Hz, and $f_3 = 9.75$ Hz. From Eqs. (3.74), it is determined that $M_1 \approx 0, M_2 = 11.7, M_3 = -15.3, N_1 = -0.1, N_2 = 7.1, N_3 = 25.1, A_1 = 402, A_2 = 2, A_3 = 1, B = 405$. Sample calculations for M_1 and A_1 are

$$M_1 = \frac{1}{1 - (3.58/7.22)^2} \left[\frac{4(500)}{8(1,000)} - \left(\frac{3.58}{7.22} \right)^2 \right] \frac{4(1,000)(68 - 26)}{4(500)(-10.5)} = -0.04$$

$$A_1 = M_2 N_3 - M_3 N_2 = (11.7)(25.1) - (-15.3)(7.1) = 402$$

From Eq. (3.79), $\dot{\alpha}_0 = 0.38$ rad/sec. Then Eqs. (3.78) give the maximum acceleration of the center-of-gravity in the Y direction of the supported body as follows:

$$\begin{aligned} \ddot{y}_{cm} &= \frac{2\pi\rho_x f_z \dot{\alpha}_0}{B} \left[\begin{aligned} &\left| \frac{d_z}{\rho_x} A_1 + \frac{d_y}{\rho_x} (N_2 - N_3) + (M_3 - M_2) \right| \frac{f_1}{f_z} \\ &+ \left| \frac{d_z}{\rho_x} A_2 + \frac{d_y}{\rho_x} (N_3 - N_1) + (M_1 - M_3) \right| \frac{f_2}{f_z} \\ &+ \left| \frac{d_z}{\rho_x} A_3 + \frac{d_y}{\rho_x} (N_1 - N_2) + (M_2 - M_1) \right| \frac{f_3}{f_z} \end{aligned} \right] \\ &= \frac{724 \text{ in./sec}^2}{405} \left[\begin{aligned} &\left| \frac{-21}{42} (402) + \frac{-84}{42} (7.1 - 25.1) + (-15.3 - 11.7) \right| \frac{3.58}{7.22} \\ &+ \left| \frac{-21}{42} (2) + \frac{-84}{42} (25.1 + 0.1) + (0 + 15.3) \right| \frac{6.02}{7.22} \\ &+ \left| \frac{-21}{42} (1) + \frac{-84}{42} (-0.1 - 7.1) + (11.7 - 0) \right| \frac{9.75}{7.22} \end{aligned} \right] \\ &= 286 \text{ in./sec}^2 = 0.74g \end{aligned}$$

In a similar manner:

$$z_{cm} = 1,580 \text{ in./sec}^2 = 4.09g$$

$$\ddot{\alpha}_m = 45.9 \text{ rad/sec}^2$$

REFERENCES

1. Avallone, E. A., and T. Baumeister, III (eds.): "Marks' Standard Handbook for Mechanical Engineers," 10th ed., The McGraw-Hill Companies, Inc., New York, 1996.
2. Housner, G. W., and D. E. Hudson: "Applied Mechanics-Dynamics," 2d ed., D. Van Nostrand Company, Inc., Princeton, N.J., 1959.
3. Beer, F. P., and E. R. Johnston: "Vector Mechanics for Engineers: Dynamics," 5th ed., McGraw-Hill Book Company, Inc., New York, 1988.
4. Boucher, R. W., D. A. Rich, H. L. Crane, and C. E. Matheny: *NACA Tech. Note* 3084, 1954.
5. Woodward, C. R.: "Handbook of Instructions for Experimentally Determining the Moments and Products of Inertia of Aircraft by the Spring Oscillation Method," *WADC Tech. Rept.* 55-415, June 1955.
6. Vane, F. F.: "A Guide for the Selection and Application of Resilient Mountings to Ship-board Equipment—Revised," *David W. Taylor Model Basin Rept.* 880, February 1958.
7. Smollen, L. E.: *J. Acoust. Soc. Amer.*, **40**:195 (1966).
8. Lewis, R. C., and K. Unholtz: *Trans. ASME*, **69**:813 (1947).
9. Taylor, E. S., and K. A. Browne: *J. Aeronaut. Sci.*, **6**:43 (1938).
10. Browne, K. A.: *Trans. SAE*, **44**:185 (1939).
11. Derby, T. F.: "Decoupling the Three Translational Modes from the Three Rotational Modes of a Rigid Body Supported by Four Corner-Located Isolators," *Shock and Vibration Bull.*, **43**, pt. 4, June 1973, pp. 91-108.